J. Indian Inst. Sci., July–Aug. 1995, 75, 403–430.

Modelling and predictability studies of the tropical coupled ocean–atmosphere system

B. N. GOSWAMI
Centre for Atmospheric Sciences, Indian Institute of Science, Bangalore 560 012, India.

Received on April 26, 1994.

Abstract

A series of studies on the predictability of the tropical coupled ocean–atmosphere system have been performed at the Centre for Atmospheric Sciences. The results provide the first estimate of the upper limit on the predictability of the coupled system. A new parameterization of the large-scale part of the convective heating in the atmosphere developed at the Centre has led to the development of a simple low-cost model for the atmospheric surface winds which is suitable for coupled modelling studies.

Keywords: Short-term climate prediction, El Nino and Southern Oscillation, coupled ocean–atmosphere system, upper limit on predictability, model for surface winds.

1. Introduction

The ability to predict tropical 'weather' (such as tropical cyclones and monsoon depressions, etc.) and tropical 'climate' (such as large-scale floods and droughts) has tremendous social–economic impact. However, the atmosphere and the coupled ocean–atmosphere system are extremely complex physical systems which make the prediction of tropical weather and climate a very challenging task. The atmosphere and the coupled ocean–atmosphere system may be represented by a set of equations that include certain approximations of some of the physical processes such as radiative heating, convective heating associated with clouds, boundary-layer turbulent fluxes of heat, momentum and mass, etc. With initial conditions defined by observations, such a set of equations or a 'model' may be integrated forward in time using a powerful computer. As we improve our understanding of these physical processes and include better representation of them, the model improves. As the model and the initial data get refined, we can expect our ability to predict the atmospheric system to improve. In fact, this is what has happened in numerical weather prediction (NWP). It started in the late fifties using the first computer ever built. In those early days of NWP, useful prediction of the weather in the middle latitude could be made only one day or so in advance. During the last three decades, tremendous progress in computer technology, better understanding of the physical processes of the atmosphere and better collection of data have led to a prediction system with useful predictive skill up to seven days in advance in the middle altitudes. With improved models and improved specification of the initial conditions, what limits our ability to predict these systems? This question was first addressed by Lorenz[1]. Using a

simple model he showed that small errors in the initial conditions would double in about three days. Keeping in mind some of the intrinsic limitations of the observing system, this puts a limit of two to three weeks on our ability to predict the weather. This limit, often known as the 'limit on deterministic predictability', has now been confirmed using more sophisticated models. This limit is governed by the instabilities and nonlinearities of the system. The instabilities make the initial error grow in time while the nonlinearities help the errors to reach a saturation level keeping the system within certain bounds. Thus, along with the progress in NWP, quantitative estimates of the predictability of the weather have also been established.

In contrast to the tremendous strides made by NWP, the climate prediction efforts using deterministic models are still in early stages. For a while the limit on deterministic predictability acted as a conceptual barrier for deterministic climate prediction. It was thought that no useful prediction beyond this limit could be achieved. However, it was demonstrated by Charney and Shukla[2] that although the instantaneous state of the atmosphere (or the weather) may not be predictable beyond 2–3 weeks, the climate or the statistical properties of the atmosphere (such as time and/or space means) may still be predictable beyond this limit. This is possible because the climate is governed by low-frequency planetary-scale flow patterns. If these low-frequency (LF) planetary-scale flow patterns were solely governed by internal dynamics or instabilities of their own scale or scale interactions with the high-frequency synoptic disturbances, then there will not be much hope for predictions beyond the limit on deterministic predictability. However, these LF planetary-scale patterns are also expected to be governed to a large extent by the forcing associated with slowly varying boundary conditions such as sea surface temperature (SST), soil moisture, snow cover, etc. This slowly varying forcing provides significant coherent changes in the planetary scales at LF, leading to potential predictability of the space–time averages. This and some subsequent studies provide the conceptual basis for climate prediction.

In this paper, we shall address the question of predictability of the tropical climate in the interannual time scale. In these time scales, the tropical climate variability is dominated by the El Nino and Southern Oscillation (ENSO) phenomenon. This is an irregular oscillation associated with very large scale simultaneous changes in the tropical atmosphere and the tropical ocean (primarily, the Pacific Ocean). The atmospheric component of the ENSO is known as the Southern Oscillation (SO), whose primary manifestation is a see-saw in the surface pressure between the southeast Pacific subtropical high and the region of low-pressure stretching across northern Australia to western Africa. The oceanic component known as the El Nino (EN) manifests itself in many oceanic fields, for example, as decrease in the western Pacific sea level and increase in the same in the eastern Pacific and large-scale warming of the equatorial eastern Pacific. As an example, Fig. 1 shows the time series of one index of the SO and another index of the EN. Several

FIG. 1. Monthly mean time series of: (a) classical index of Southern Oscillation, *i.e.*, the pressure difference between Easter Island and Darwin in mb, (b) sea-surface temperature anomalies in the eastern equatorial Pacific region (20 S–20 N, 80 W–180 W) in degrees C. The thick line in (a) represents a 12-month running mean, and in (b) 15-month weighted average.

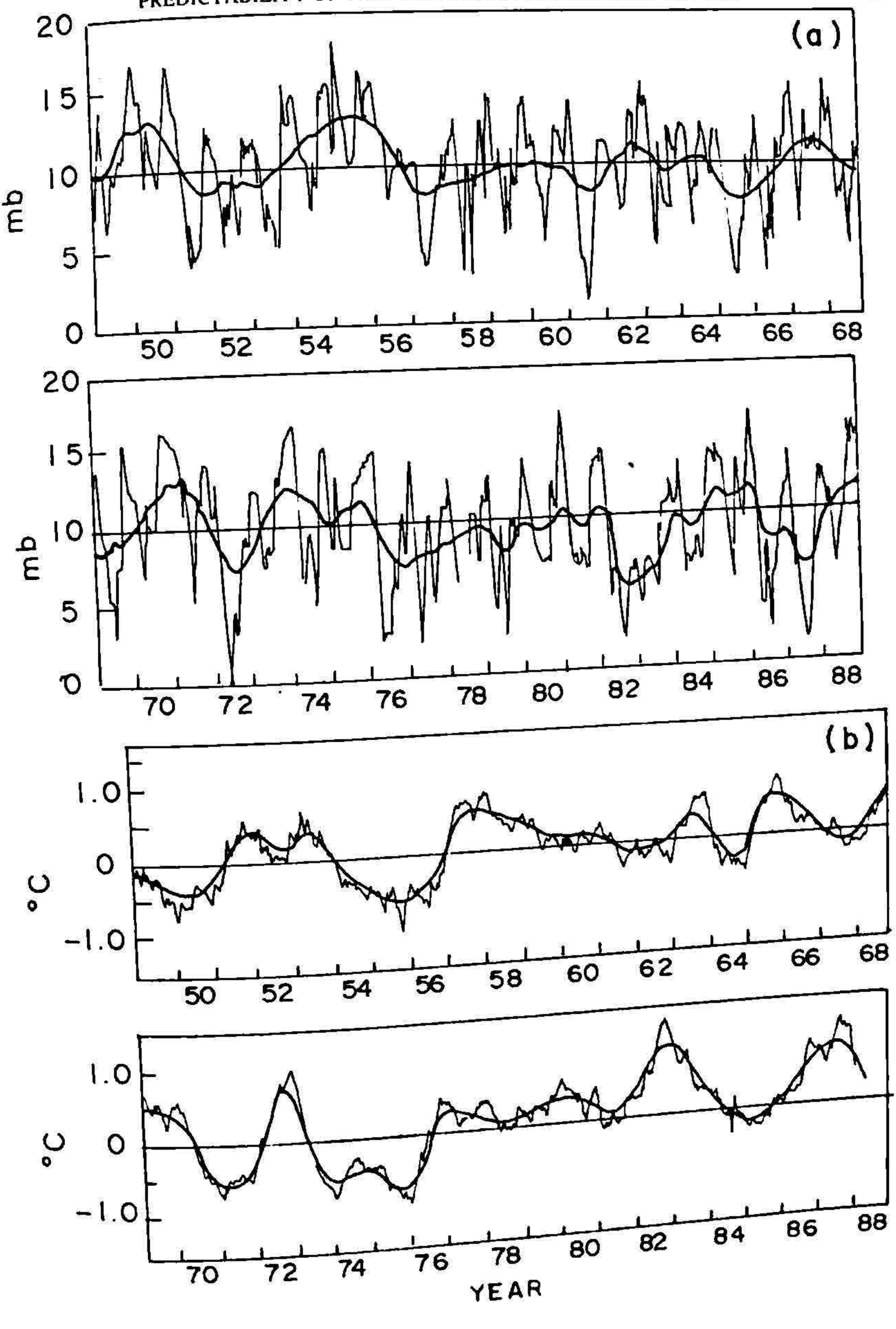
(a)
mb
20
15
10
5
0
50 52 54 56 58 60 62 64 66 68
70 72 74 76 78 80 82 84 86 88
(b)
°C
1.0
0
-1.0
50 52 54 56 58 60 62 64 66 68
70 72 74 76 78 80 82 84 86 88
YEAR

features are noteworthy. High-frequency intraseasonal oscillations (light curve) are superimposed on a dominant low-frequency oscillations (heavy curve) of both the atmosphere and the ocean. There is a very high coherence between the atmospheric low-frequency oscillation and the oceanic low-frequency oscillation. However, the high-frequency oscillations of the two systems are not well correlated. The low-frequency oscillation is quite irregular but seems to have a preferred periodicity of about four years. This is seen in Fig. 2, where the power spectra of SO and EN indices are shown. It is clear that there is a dominant peak around four years but it is a broad-band spectrum indicating the already noted aperiodicity. It was Bjerknes[4] who first suggested that the low-frequency coherent fluctuations in the tropical atmosphere and the ocean may arise as a result of unstable air–sea interactions. The atmospheric surface winds drive the oceanic surface currents that redistribute the heat in the ocean, leading to a new distribution

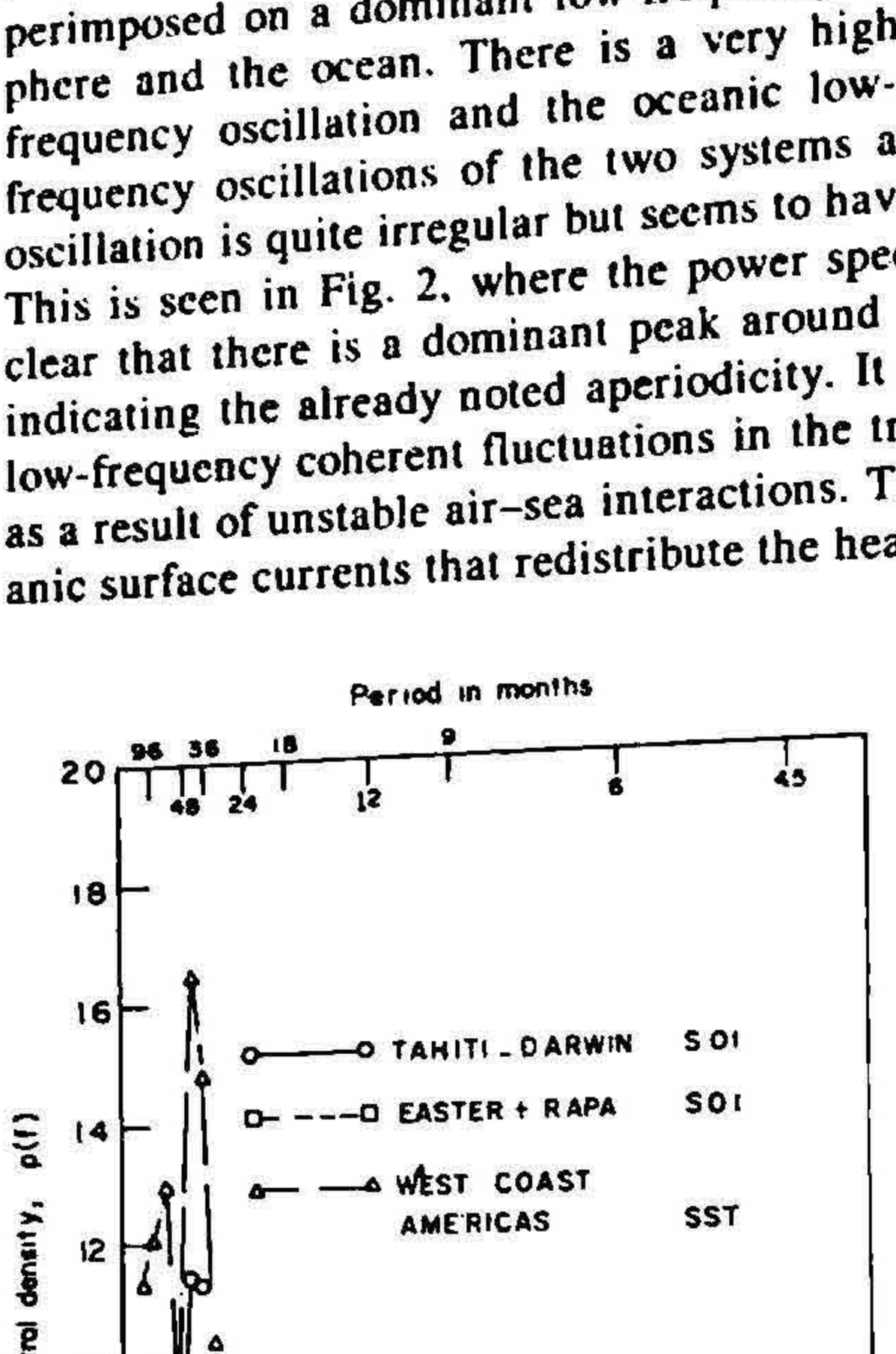

FIG. 2. The spectra for mean monthly anomaly time series (September 1953–December 1974) for Tahiti minus Darwin-normalized surface pressure difference, Easter Island plus Rapa surface pressure and SST anomalies near upper Peru coast (4–12 S) (after Rasmusson and Carpenter[3]).

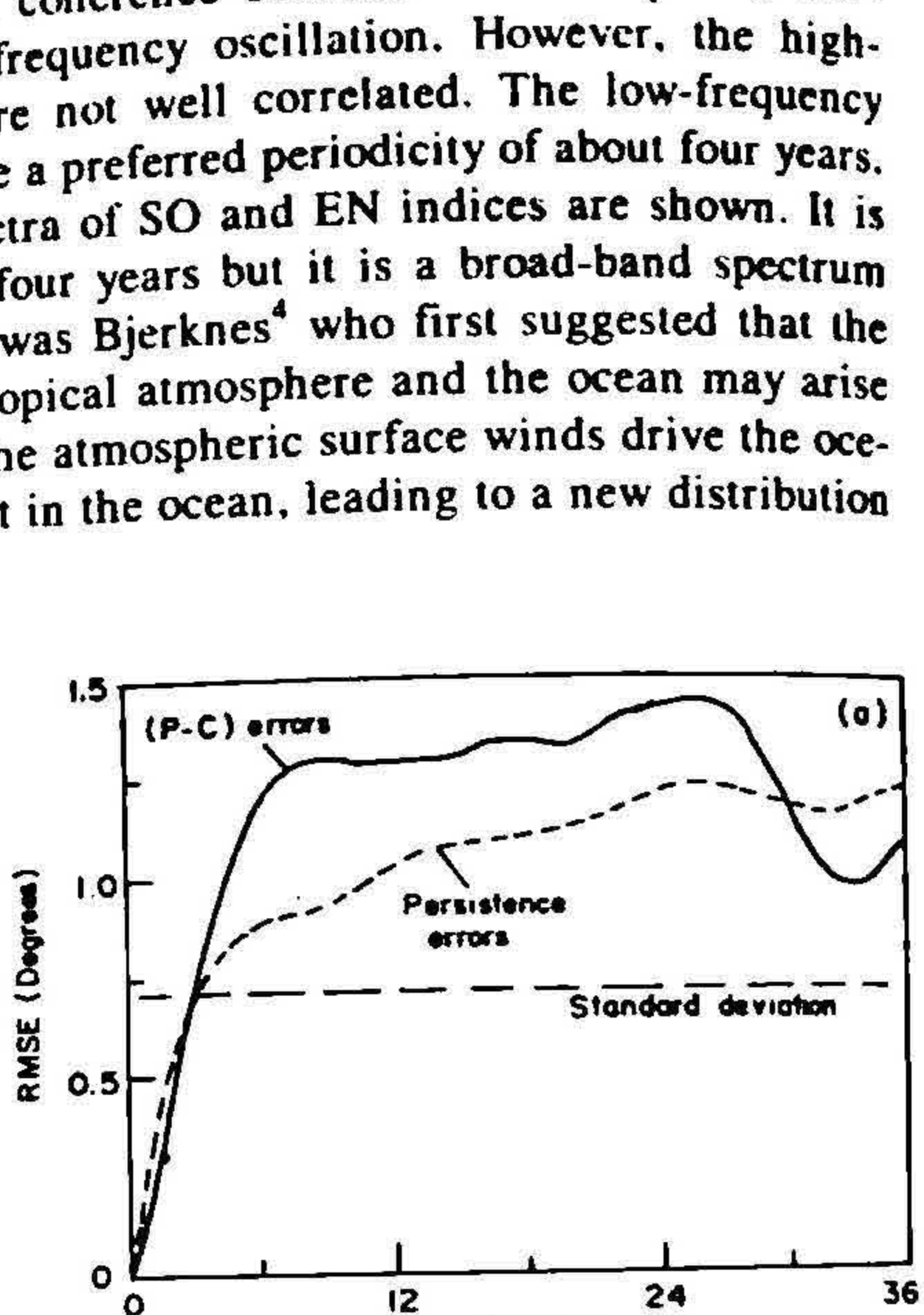

FIG. 3. (a) RMS prediction minus control (P–C) errors for SST anomalies averaged over the NINO3 region (5 S–5 N, 150 W–90 W) using all 181 predictions (solid). The persistence errors as well as the standard deviation of the control NINO3 SSTA are also shown. (b) correlation coefficients (r) between the predictions and verifications of NINO3 SSTA from the control.

of SST. The SST in turn modulates the atmospheric convective heating that drives the surface winds. Under certain conditions, an increase in SST can lead to enhancement of the surface winds such that it helps to enhance the SST further. It was only in the mid-eighties when several studies[5–7] showed that even though the linear atmosphere and the linear ocean are independently stable, the coupling may give rise to a low-frequency unstable mode in the tropical coupled ocean–atmosphere system under certain conditions.

The understanding of such coupled air–sea interactions has emerged from knowledge gained from studies of the individual uncoupled systems. For example, studies of atmospheric response to a given heat source[8, 9] have shown that it generates westerly anomaly to the west and easterly anomaly to the east of the heat source. Oceanographic studies[10–12] have shown that the oceanic response to such a burst of westerly winds generates a downwelling Kelvin wave (one with anomalous depression of the thermocline) that propagates to the east and an upwelling Rossby wave that propagates to the west. At this point one could ask two questions. Firstly, can such air–sea interactions give rise to climate fluctuations in the interannual time scale? Secondly, under what conditions do such air–sea interactions lead to a positive feedback?

The answer to the first question is in the affirmative due to three special characters of the tropical ocean–atmosphere system. (a) The mean SST in the tropical region is high (>26.5°C) in large regions. A small increase in SST is capable of generating large increase in evaporation and hence the availability of moisture in this region. (b) Due to the conditionally unstable nature of the tropical atmosphere, such available moisture can be converted to tropospheric heating through cumulus convection. (c) The equatorial ocean allows a free Kelvin wave with phase speed of about 2 m/s. The gravest meridional mode Rossby wave has phase speed one-third that of the Kelvin wave. For these long waves, the phase speed and the group speed tend to be equal. A Kelvin wave packet would take 2–3 months to cross a basin of the size of the Pacific Ocean while the gravest Rossby wave would take 6–9 months to cross the same. Thus, these wave packets can redistribute heat in the equatorial region in the time scale of a season to a few years. In the extratropics, the free Kelvin wave does not exist. Moreover, the phase speed of the Rossby waves goes inversely as the square of the distance from the equator. As a result, the time scale of SST changes in the extratropics due to wave dynamics is much longer. Regarding the second question, detailed analysis of the energetics of the linear coupled system[6, 7] has shown that if the surface wind convergence produced by heating in the atmosphere forces oceanic currents such that convergent atmospheric winds overlay convergent oceanic currents, a positive feedback could take place. It has been shown[13] that the mean conditions in the central and eastern Pacific are conducive for such a coupled instability.

Meteorologists have shown[14] that the low-frequency variations in the tropical atmosphere are primarily driven by the forcing associated with the observed low-frequency variations in the tropical SST. Similarly, oceanographers[15] have shown that the low-frequency oceanic variations in the tropics are mainly driven by the observed surface wind variations. These studies underlined the fact that for simulating the interannual variability in the tropics, the coupled ocean–atmosphere system has to be modeled. These two developments and the discovery of the existence of an LF unstable coupled

mode have led to considerable efforts during the last decade on simulating the observed tropical interannual variability using coupled models of various complexity. These range from simple anomaly models[16] to complex coupled general circulation models (CGCMs)[17-19]. However, most of these coupled models suffer from some systematic errors that often lead them to drift to their own climate[20,21]. An initial small error in the atmospheric component resulting in a small error in the surface winds introduces a small error in the SST which can amplify in time due to the existence of the unstable air–sea interactions in the system. This makes the modelling of the tropical coupled ocean–atmosphere a challenging task.

In such a coupled system, the concept of slowly varying boundary forced predictability is not applicable as the boundary condition for one component is an internal variable for the other component. Thus, the potential predictability, if at all it exists, must result entirely from the internal dynamics of the coupled system. Since the system has some LF internal oscillations (such as the quasi-four-year ENSO oscillation), these oscillations themselves provide the basis for extended range predictability of the coupled system. As mentioned earlier, efforts to predict these interannual oscillations using coupled models have begun[22,23]. However, all these models are in the their early stages of development. Moreover, the initial conditions for these coupled models require surface and subsurface data from the world ocean. At present, this is poorly represented. As the models improve and the data assimilation system for the coupled system also improves, we can expect our ability to predict ENSO also to improve. Unlike the NWP, however, there was no quantitative estimate of the limit on the predictability of the tropical coupled system. In this paper, we summarize a series of studies that we conducted to provide the first estimate of the theoretical limit on the predictability of the coupled system and attempts to identify the factors that may be responsible in determining this limit.

Conceptually, any long-range predictability of the ENSO may be expected due to the dominance of the four-year periodicity, while the limit on this predictability would result from the nature of the aperiodicity of the four-year oscillation. Therefore, there is a need to understand the origin of the quasi-four-year oscillation in the coupled system as well as the origin of its aperiodicity. Both these are subjects of active research currently. A plausible scenario for the four-year periodicity has been proposed by Suarez and Schopf[24] and Battisti and Hirst[25]. Let us assume that a westerly wind burst is triggered by atmospheric disturbances in the central Pacific. It is well known from oceanographic studies that such a wind burst produces a downwelling Kelvin wave packet that propagates to the east. This downwelling Kelvin pulse triggers the coupled instability in the eastern Pacific and increases the SST (warm event). At the same time, an upwelling signal is excited in the central Pacific that propagates to the western boundary in the form of the gravest meridional Rossby wave, gets reflected from the western boundary, returns to the warming area as an equatorially trapped upwelling Kelvin wave and destroys the downwelling signal. Some of these upwelling pulses take the SST to a decreasing phase. During the decreasing phase, downwelling Rossby wave packets are generated that propagate to the western boundary, return as downwelling Kelvin wave and initiate the neat growth phase of instability. Thus, a balance between the positive feedback associ-

ated with the coupled instability and the negative feedback associated with the reflection of the Rossby waves from the western boundary can lead to an oscillation. The period of the oscillation is determined by a combination of the growth rate of the instability (determined by various thermodynamic processes in the region) and the travel time of the Rossby–Kelvin pair back to the warming region (determined by equatorial wave dynamics and the size of the basin). The size of the Pacific basin being large, it can sustain such an oscillation. On the other hand, in a small basin like the Indian Ocean, even if the coupled instability exists, the reflected Rossby waves kill any warming signal before they can develop into any appreciable size. This mechanism, often referred to as the 'delayed oscillator mechanism', can be represented by a simple analog equation given by

$$F_t = aF(t) - bF(t - \tau) - cF^3(t),$$

where F represents the temperature anomaly, a, the growth rate of the coupled instability, b, the strength of the negative feedback associated with the Rossby wave reflection, c, the strength of the nonlinearity associated with the perturbation upwelling and τ, the delay time associated with the reflected Rossby wave. Although this seems to be a plausible mechanism, it appears that other mechanisms could as well produce the oscillation in the real coupled system, and in some coupled GCMs. While the mechanism for the four-year oscillation is still being debated, the cause for the periodicity is even more unclear. In this paper, we shall present a conceptual model for the aperiodicity of the tropical coupled system.

As we mentioned earlier, for the coupled models to be useful for climate predictions, it is essential that the climate drift be minimized. A prerequisite to achieve this goal is that the individual components of the coupled system simulate the observations accurately when forced by observed boundary conditions. In other words, the atmospheric component must simulate the surface winds correctly when forced by the observed SST and the ocean component must simulate SST correctly when forced by the observed surface wind stresses. To gain insight regarding the maintenance of the tropical surface winds, we have examined the simulation of the surface winds by an atmospheric GCM. We have also developed a very simple model for the tropical surface winds that is capable of simulating them almost as well as the GCM at a fraction of the cost. A summary of these studies will also be discussed in this paper. In Sections 2, 3 and 4, we summarize the results of our predictability studies while in Section 5 we discuss some results on simulation of the surface winds in the tropics with a complex atmospheric general circulation model (AGCM) as well as with a simple linear model.

2. Predictability studies

Coupled models are now being used for experimental forecasts of ENSO events[21,22,26]. However, a quantitative estimate of the forecast skill of these models as well as an estimate of the theoretical limit on the predictability of such climate fluctuations are lacking. In this section, we present the results of our investigation with a coupled model to estimate the theoretical limit on the predictability of the coupled system (analogous to deterministic limit on the predictability of the weather).

In this study we used the coupled model developed by Cane and Zebiak[16,22] (hereafter referred to as the CZ model) and carried out a series of 181 three-year forecasts[27]. This is one of the simplest coupled models that has proved successful in simulating many features of the observed interannual variability in the tropics. The model is an 'anomaly' model in which the climatological mean annual cycle is prescribed and the model determines the evolution of the anomalies. The atmosphere is global in extent but the ocean is a rectangular basin representing the Pacific Ocean. The main nonlinearity in the model comes from the advection of the temperature anomalies. For initiating coupled predictions, coupled initial conditions consisting of both atmospheric and oceanic observations are required. While operational data assimilation and analysis systems are available for the atmosphere, the same are currently not available for the coupled system. This is mainly due to the nonavailability of oceanic observations. Therefore, a rather simple analysis scheme is used to generate the initial conditions for our coupled forecasts. We have reasonable surface wind observations over a long period of time. It is also known that the dynamics of the upper layers of the ocean is mainly driven by surface winds. Therefore, if we have a reasonably good ocean model which is forced by the observed surface winds over a long period of time, we can expect the model to generate reasonably good history for the oceanic currents and SST. Thus, we carried out a control run in which the ocean model was forced with observed surface winds from January 1964 till May 1988. A comparison of the model-simulated anomalies with observations[27] shows that the model does a good job simulating the observed El Nino events. Allowing the ocean to come to equilibrium with the observed winds, we save all the oceanic fields from January 1970. The atmospheric response to SST anomalies corresponding to any month of the control run together with the oceanic fields for that month gives us a balanced initial condition for the coupled model. In this way, three-year coupled forecasts starting with initial conditions form January 1970 till December 1985 are made. Here the model is run in the coupled mode in which the atmospheric model generated winds feedback to the ocean to determine the future evolution of the SST. The error in the forecasts is measured by the difference between the coupled forecasts and the control run. It is found that the forecasts depend sensitively on the initial conditions.

A gross measure of the skill of the forecasts may be obtained form the root mean square error (RMSE) averaged over all the forecasts. It is seen from Fig. 3 that the current average skill of the model is not more than four months as by this time errors become larger than those for persistence forecasts. However, this is somewhat misleading. In Fig. 4 we show a series of six pairs of forecasts starting from two consecutive months in each case. As seen from Fig. 4, the skill of forecasts starting with some initial conditions is far better than this conservative estimate. It is generally found that forecasts initiated from boreal fall/winter have much better skill than those initiated from boreal spring/summer.

To estimate the theoretical limit on the predictability, we carried out 151 pairs of 'identical twin' experiments, each for a duration of 15 years. Each pair is identical in all aspects except for one which contains a small perturbation in the initial condition. The divergence of the two forecasts in the pair represents growth of small errors in the initial

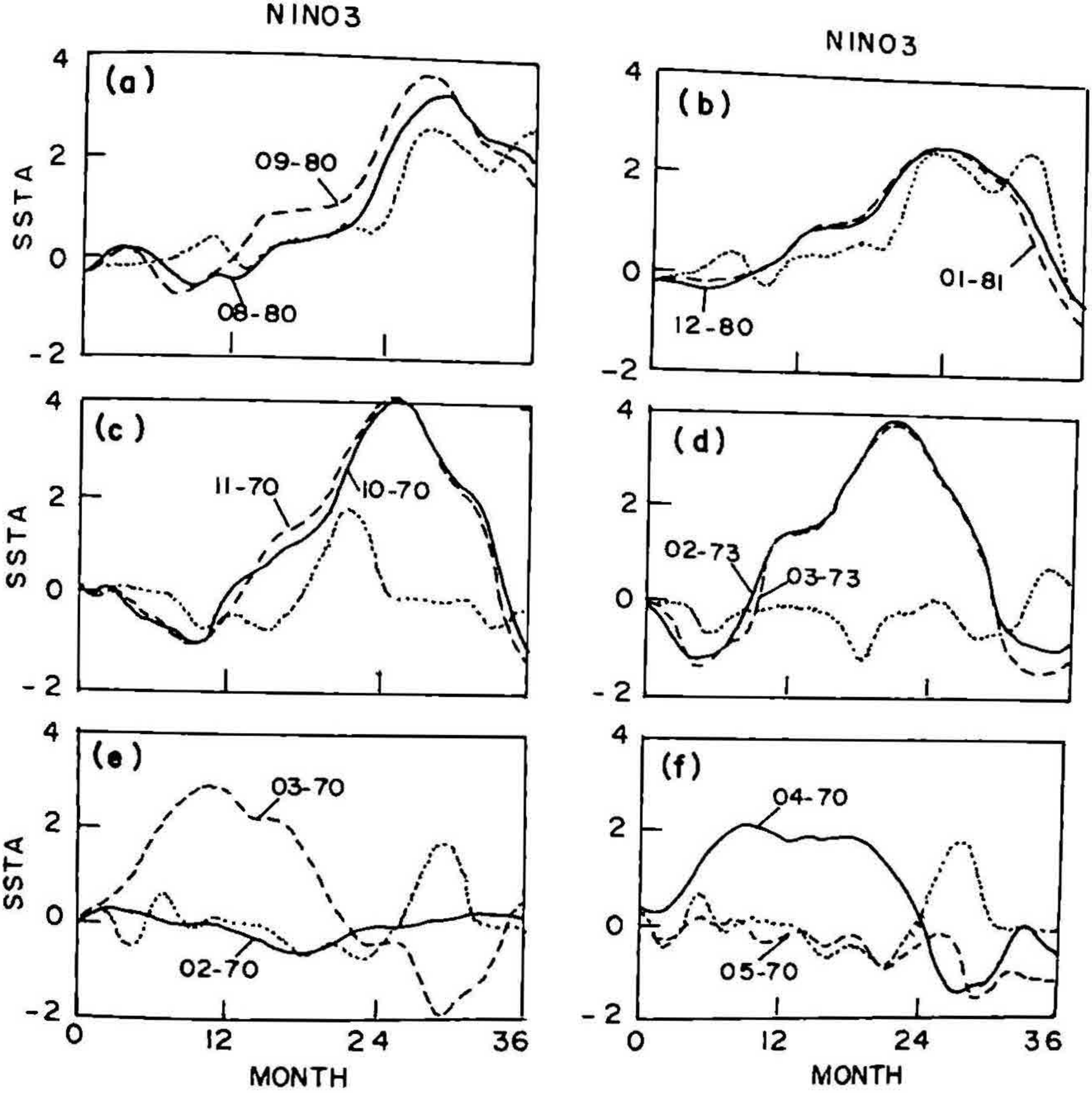

FIG. 4. Verification of six pairs of subjectively selected predictions of NINO3 SSTA starting from two consecutive months. The dotted curve is the control in each panel and the solid and the dashed curves are the two predictions. The starting months are shown as mo–yr.

conditions assuming that the model is perfect. The growth of such errors (Fig. 5) shows that it is governed by two time scales. Empirical fitting of the curve with two different error growth processes indicates one fast time scale with error-doubling time of about 5 months and another slow time scale with error-doubling time of about 15 months. Thus, if one could identify the initial conditions that would support only the slow error growth, one could, in principle, hope for prediction of the ENSO events one-and-a-half to two years in advance. The question is, how do we suppress the fast growth of errors in the initial conditions? If we could answer this question, we could hope to develop

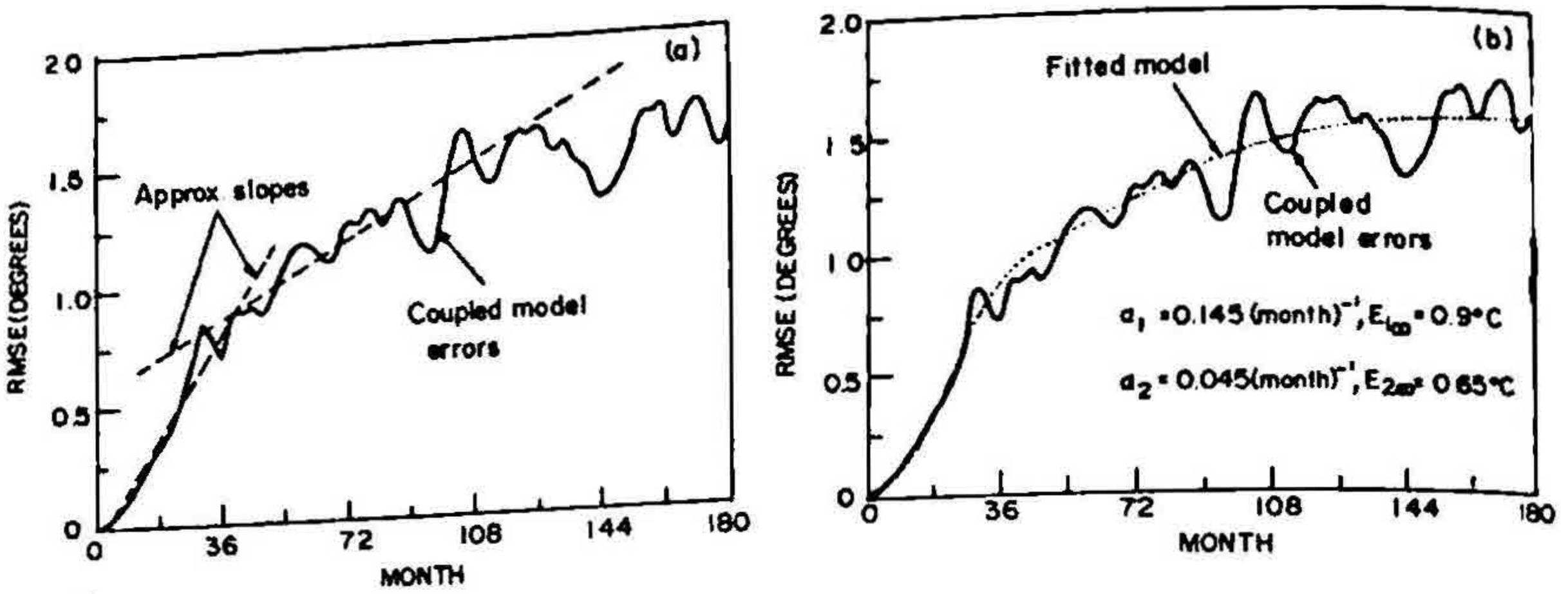

FIG. 5. Empirical model for growth of small errors. (a) rms error from 151 identical twin experiements due to small random initial perturbations in the surface winds. The dashed curve approximately shows the two different slopes of the error curve. (b) the fitted model for the error curve in (a).

'initialization' schemes for coupled predictions analogous to 'initialization' schemes for NWP. Before we could do this, however, we have to understand the dynamical factors that govern the fast growth of errors in the initial conditions.

To gain some insight regarding this, we carried out a series of sensitivity experiments with the CZ model. The basic variability of the model is aperiodic but has a dominant four-year periodicity. We argued that if the variability was periodic, the predictability will be very high. Therefore, the factors that give rise to aperiodicity in the model must also be responsible for the fast error growth. Our experiments with the coupling processes showed[28] that for the standard set of parameters of the CZ model, aperiodicity of the model may be attributed to the 'convergence feedback' associated with the atmospheric heating of the model (denoted by β). An initial increase in the SST gives rise to atmospheric heating. The heating generates anomalous surface convergence of the moisture, leading to strengthening of the heating. This process is termed as the 'convergence feedback'. In the absence of the convergence feedback, the model's variability is quite periodic (Fig. 6). As the strength of the coupling associated with the convergence feedback is slowly increased, the model's variability slowly changes from a periodic to an aperiodic regime (Fig. 7). The spectra (not shown) of these time series show that it goes from a line spectrum at a low value of the convergence feedback to a broad-band spectrum at a high value of the convergence feedback. Further analysis revealed that this process is a strong function of the annual cycle. Figure 8 shows that if the mean convergence is fixed at March values, the model becomes aperiodic at a very small strength of the coupling, while Fig. 9 shows that if the mean convergence field is held fixed at September values, the model tends to remain periodic until large values of the coupling strength. This is consistent with the fact that the forecasts initiated with boreal spring are associated with higher predictability. These experiments indicate that the model has a basic four-year LF oscillation and the convergence feedback introduces some new modes that interact nonlinearly with the LF mode and make it aperiodic. The

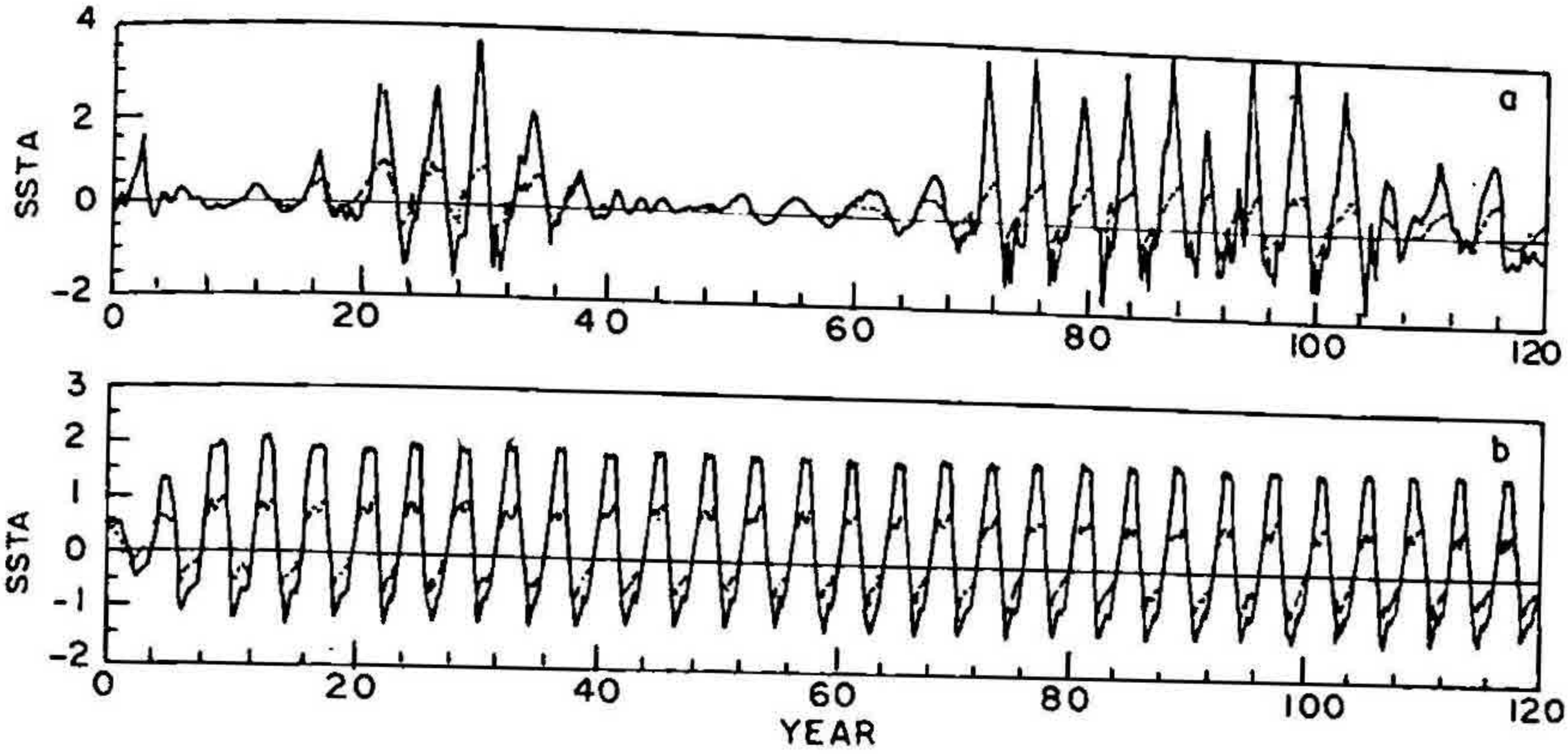

FIG. 6. The time series of area-averaged SSTA (°C) from the standard run of the CZ model for 120 years (a) with convergence feedback $\beta = 0.75$ and (b) without convergence feedback. $\beta = 0.0$. The solid curve is for NINO3 (5 S–5 N, 90 W–150 W) and the dashed curve is for NINO4 (5 N–5 S, 150 W–160 E).

next big question is to identify the coupled oscillations introduced by the convergence feedback process.

3. Stability analysis of a linear coupled ocean–atmosphere model

To answer the above question, we conducted a stability analysis of the linear coupled system in the presence of the convergence feedback[29, 30]. A dry air parcel cools due to adiabatic expansion in a region of ascending motion. However, if the moisture converged on the ascending region due to anomalous low-level convergence condense, it releases the latent heat, reducing the adiabatic cooling. Thus, the convergence feedback may be modelled as a reduction of the static stability of the atmosphere. It is shown that in the absence of the convergence feedback, the coupled model sustains only one LF unstable mode. In the presence of the convergence feedback, in addition to the LF unstable mode, a number of higher-frequency intraseasonal (IS) modes are also sustained (Fig. 10). The growth rate of these IS modes is smaller than that of the gravest LF mode. At long wavelengths, the LF mode still dominates. At shorter wavelengths, however, the LF mode is stable while the IS modes are still unstable. Therefore, at shorter wavelengths the IS modes are expected to dominate.

4. A conceptual model for the limit on predictability

The LF unstable mode together with the reflections of the Rossby waves from the western boundary is attributed to the dominant oscillation with a period of about four years. Our discovery, discussed in the previous section, indicates that the dominant long-wave LF oscillation with a period of about four years will coexist with a host of IS oscillations with shorter wavelengths. With this recognition, we propose a conceptual model for the aperiodicity in the tropical coupled system[31, 32]. It is argued that the LF oscillation, by

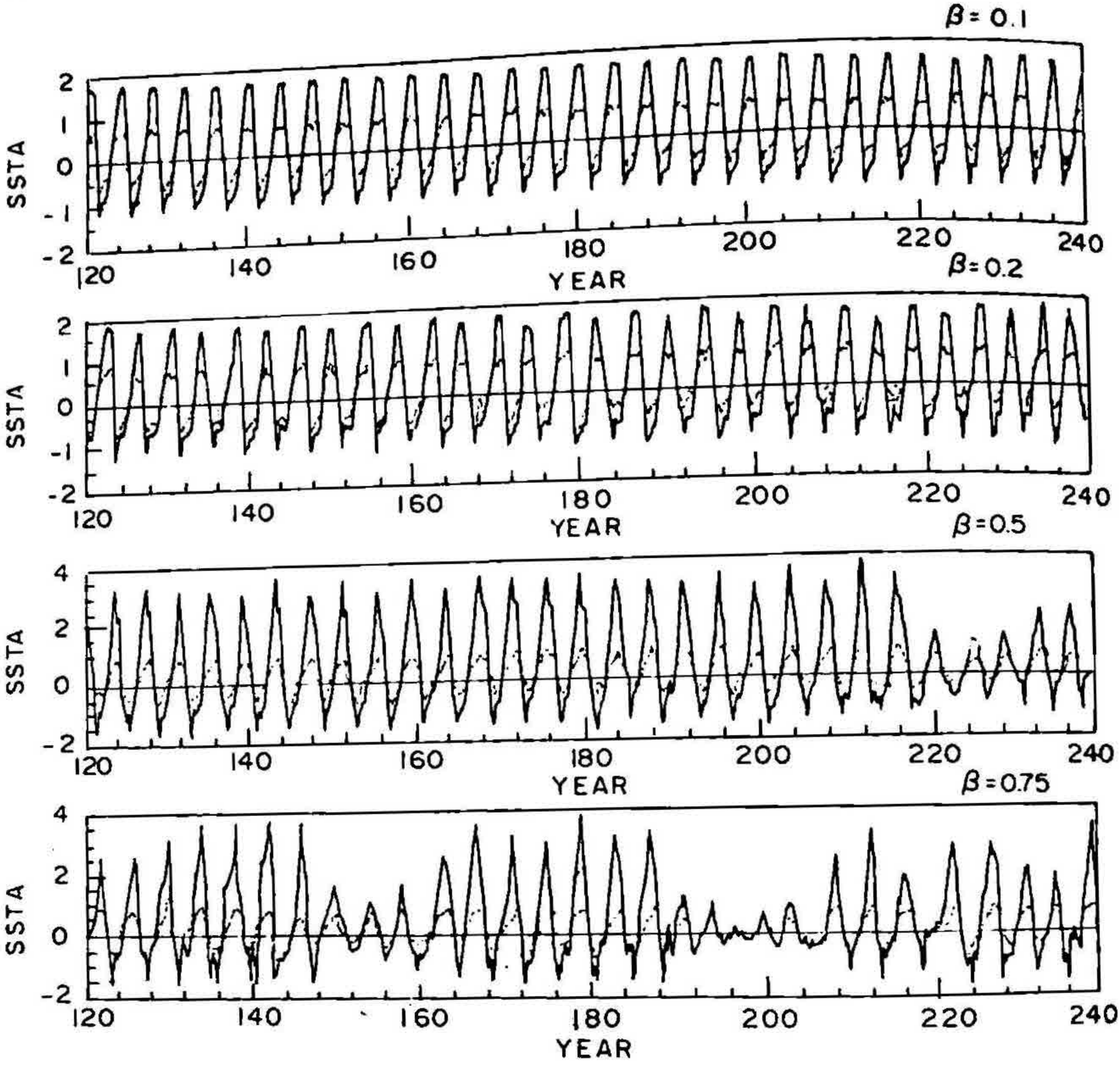

FIG. 7. Time series of the same area averaged quantities as in Fig. 6. but for four experiments with increasing strengths of convergence feedback. Each experiment was integrated for 240 years and the evolution for the last 120 years is shown in each case.

virtue of a very long characteristic length scale associated with it, may be considered as a linear oscillator. It can be shown that the equatorial Rossby number $U/\beta_0 L^2$ (near the equator the Coriolis parameter is $f \approx \beta_0 y$) for such planetary-scale phenomenon is small. As a result, the nonlinear advection is not likely to be important for the LF mode. However, the IS modes have much shorter wavelengths and for them the equatorial Rossby number is large and the nonlinearity would be important. It is then proposed that an interaction between this LF linear oscillator and the higher-requency nonlinear IS oscillations results in broadening of the LF spectrum, resulting in aperiodicity of the LF mode.

To represent the nonlinear interactions between the high-frequency waves, we choose a prototype nonlinear system used by Lorenz[33] to describe some aspects of the general

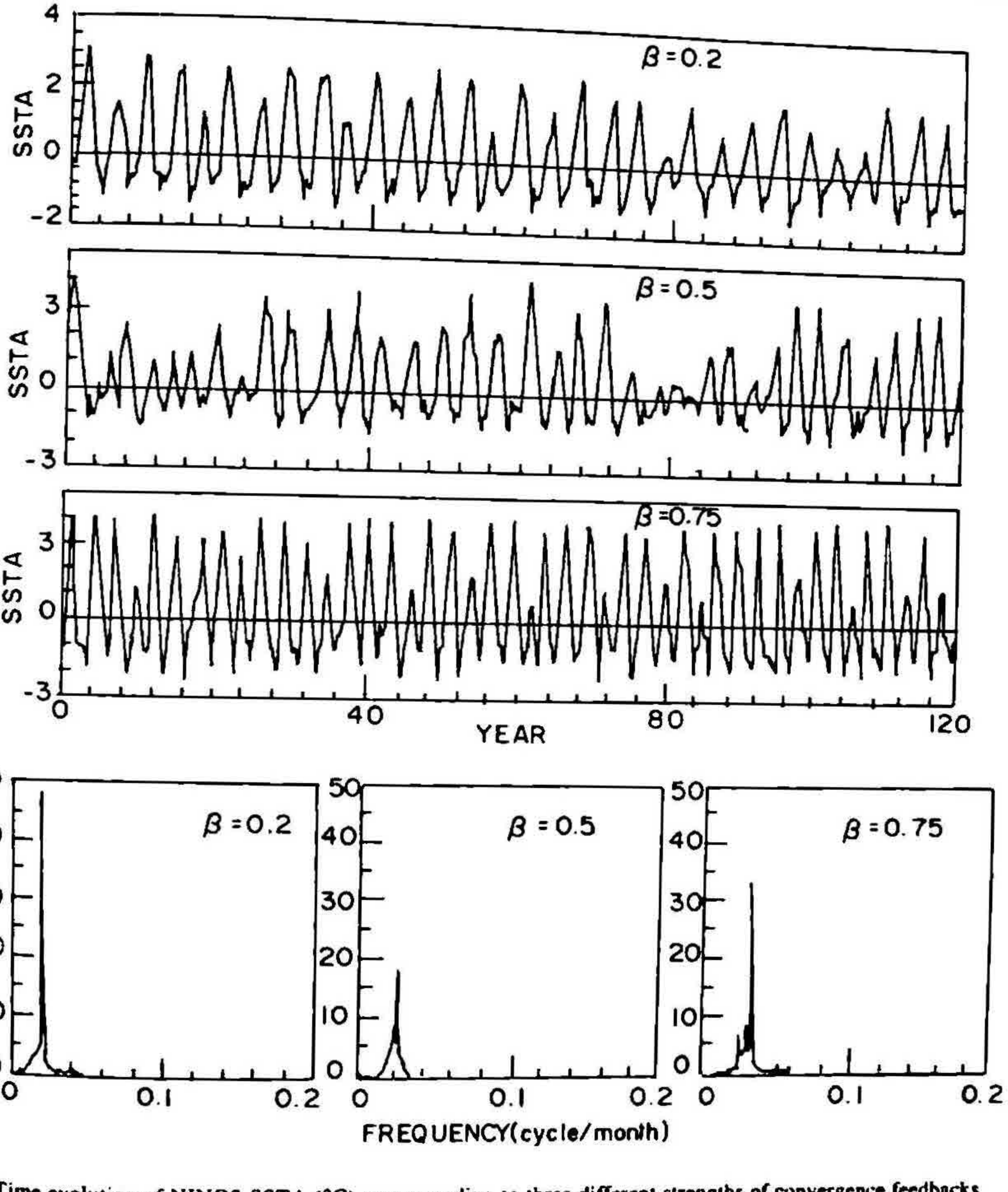

FIG. 8. Time evolution of NINO3 SSTA (°C) corresponding to three different strengths of convergence feedbacks when the mean convergence field is held fixed at March values. The other mean fields have normal annual cycle. The power spectra of the three time series are shown below (from Goswami and Shukla[28]).

circulation of the atmosphere. Coupling these nonlinear equations to a linear oscillator, the equations for the coupled system may be written as

$$\dot{X} = -Y^2 - Z^2 - \alpha X + \alpha F, \tag{1}$$

$$\dot{Y} = XY - bXZ - CY + G + \alpha P, \tag{2}$$

$$\dot{Z} = bXY + XZ - CZ + \alpha Q, \tag{3}$$

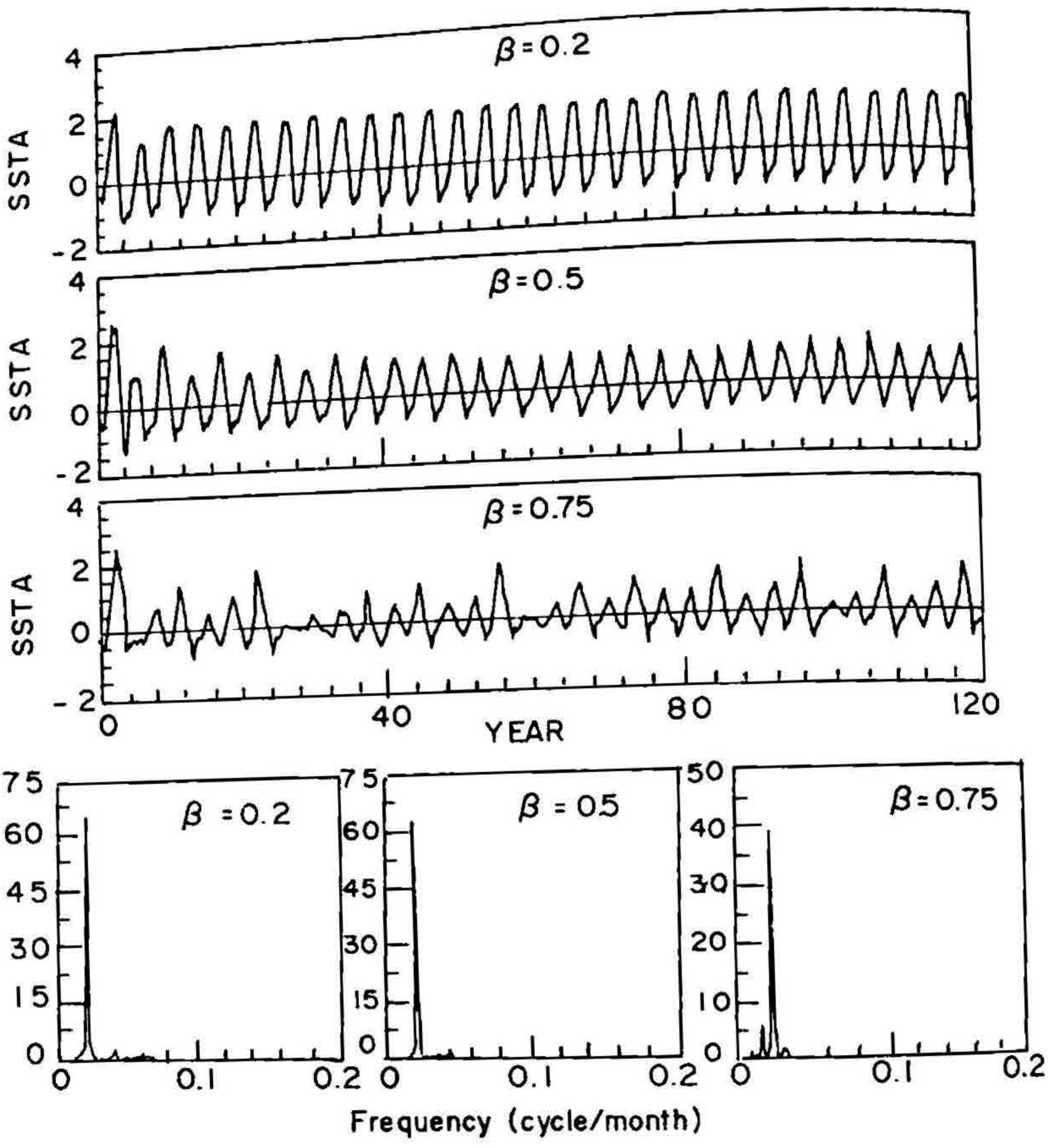

FIG. 9. Same as in Fig. 8 except when the mean convergence field is held fixed at September values (from Goswami and Shukla[28]).

$$\dot{P} = -\omega Q - \beta Y, \tag{4}$$

$$\dot{Q} = \omega P - \beta Z, \tag{5}$$

where ω is the frequency of the LF oscillator with a period of four years, p and Q are the amplitudes of the sine and cosine phases of the oscillation and α and β, the coupling strengths. Equations (1)–(3) represent the HF coupled modes while eqns (4)–(5) represent the LF mode. The typical time scale of the HF coupled modes is in the intraseasonal range. In order that the nonlinear system contains this intrinsic time scales, we have

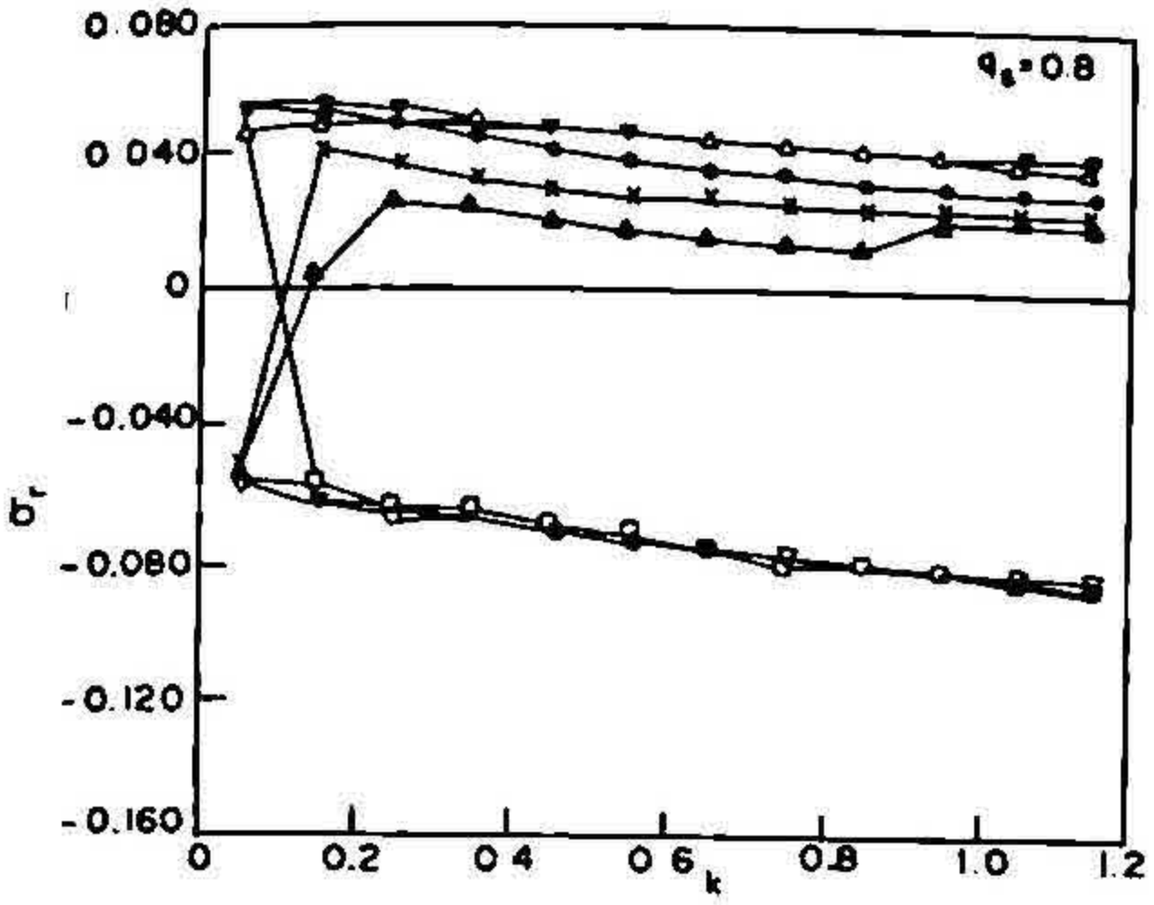

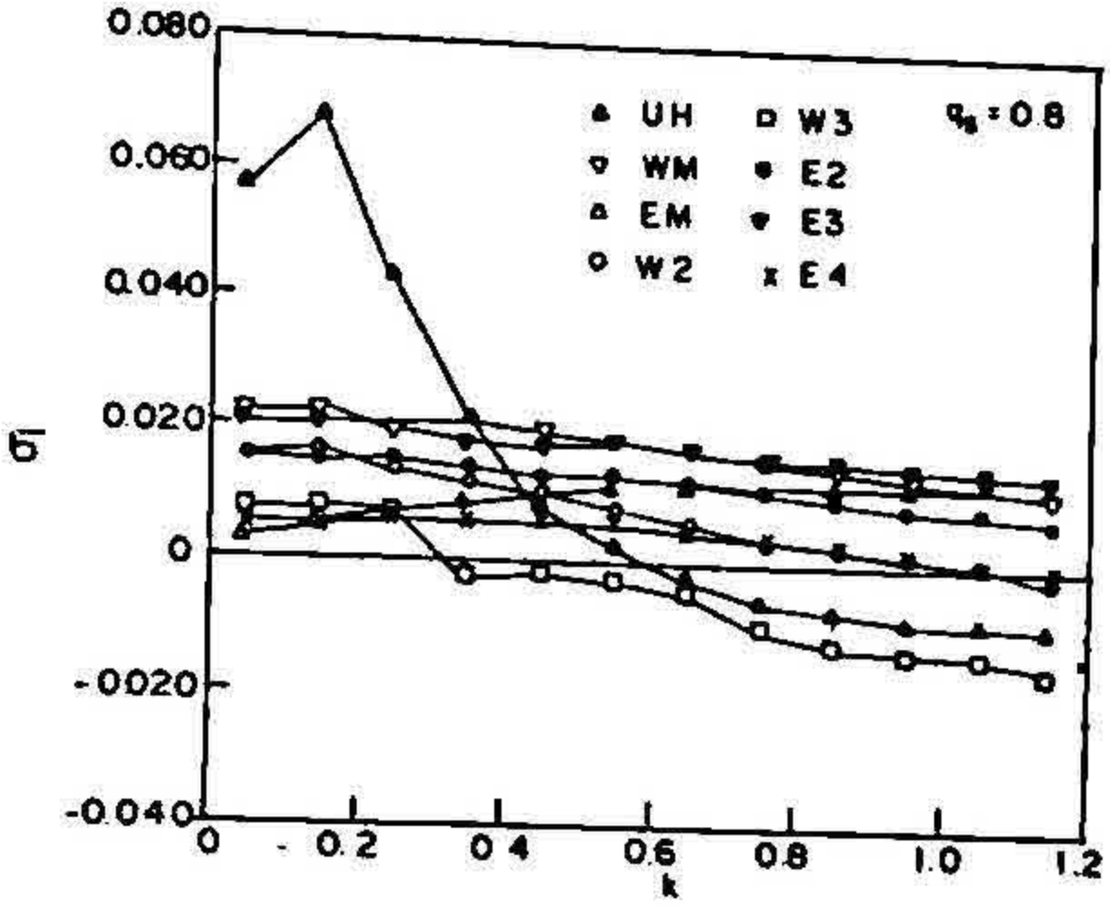

FIG. 10. Nondimensional dispersion relation (all modes) for the strength of convergence feedback, $q_s = 0.8$, implying 80% reduction of dry static stability. σ_r, σ_i and k are nondimensional real, imaginary frequencies and wavenumbers, respectively. UH, WM and EM represent the unstable low frequency mode and the maximally growing eastward and westward propagating modes. Other symbols refer to other eastward (E) and westward propagating (W) intraseasonal modes (from Selvarajan and Goswami[30]).

rescaled the original equations of Lorenz with a scaling factor C. X may be interpreted as a zonally averaged field while Y and Z may be interpreted as amplitudes of the two wave components. F and G are forcing. F may be considered as external zonally symmetric forcing (*e.g.*, solar forcing) while G may be considered as a zonally asymmetric forcing (*e.g.*, land-ocean contrast). With $C = 0.5$ the simple model time series has many characteristics similar to the observed ENSO time series[32].

When the coupling of HF to LF is weak (β small), LF remains essentially periodic. As shown in Fig. 11, with increase of coupling, LF oscillation starts becoming aperiodic. The spectra of the time series for the three increasing values of the coupling are also shown in Fig. 11. The transition from a line spectrum to a broad band one with increasing strength of coupling is reminiscent of transition to aperiodicity in the Cane–Zebiak model in the previous section. The broadening of the LF spectrum takes place in the following way. The coupling of the HF component to LF can be considered as a slowly varying forcing for the HF component. For the range of forcing involved, the HF component goes through a chaotic regime. As a result of the slowly varying forcing, an LF tail in the spectrum of the HF system is introduced. This when felt by the LF system as a forcing generates resonant response around the four-year period, leading to the broadening of the LF spectrum and its aperiodicity. The limit on the predictability of ENSO is related to how broad the spectrum of ENSO is. The above results indicate that the broadening of the spectrum and hence the limit on the deterministic predictability of ENSO depends on the strength of coupling of the HF to the LF oscillation. This conceptual model has also been used recently to propose a mechanism for the origin of the tropospheric quasi-biennial oscillation[34].

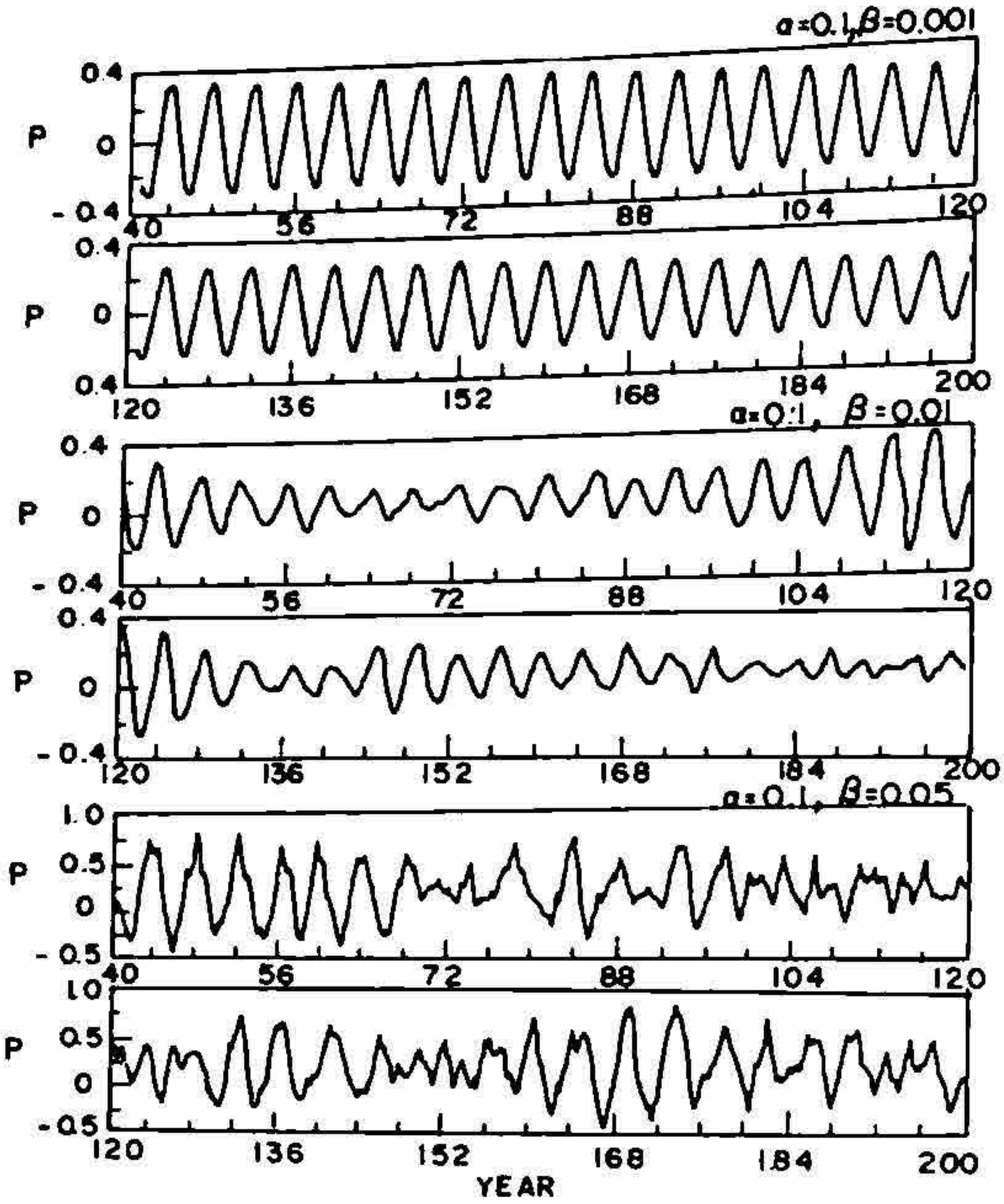

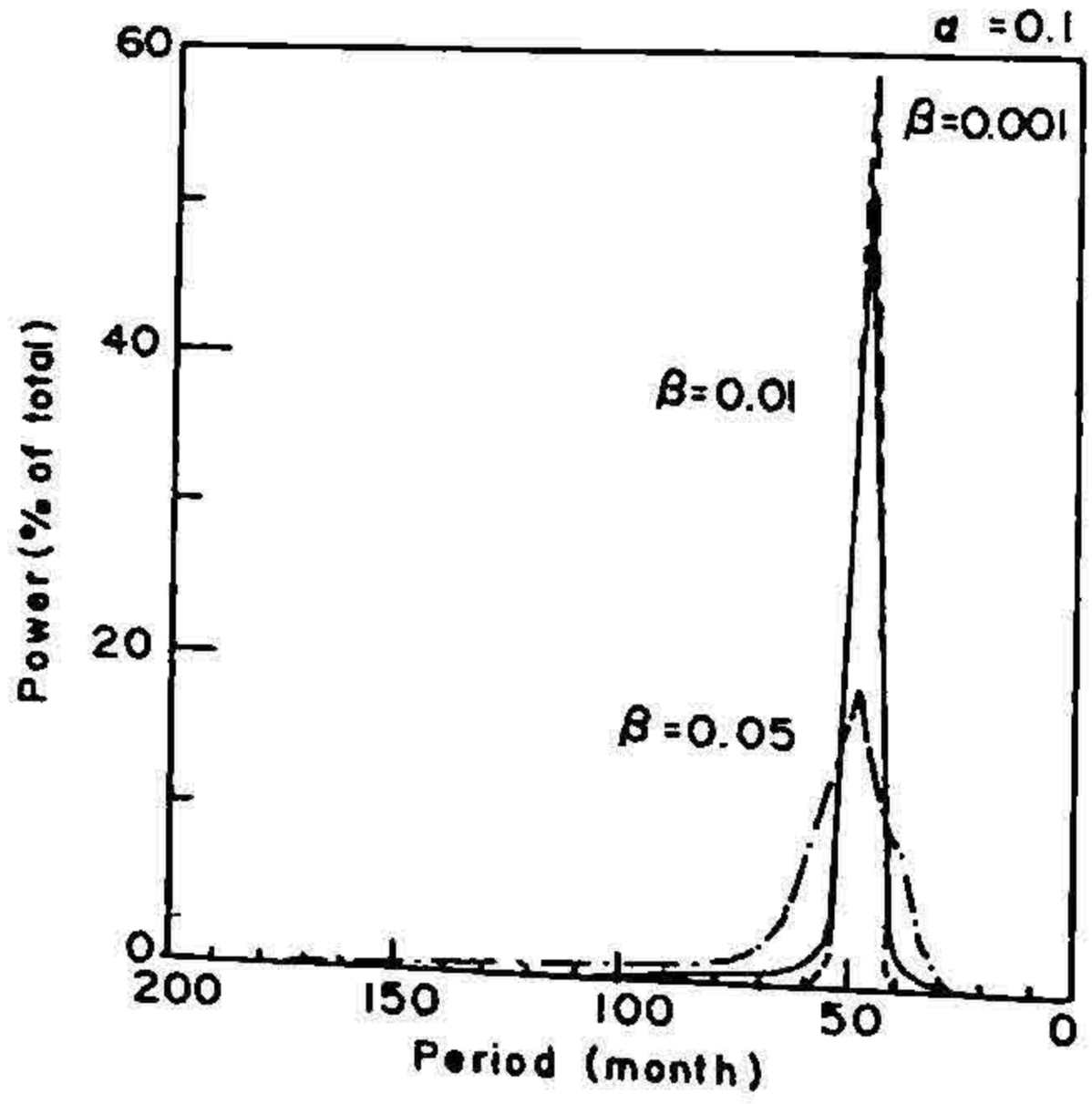

FIG. 11. 160-year time series of P from the conceptual model with $\alpha = 0.1$ and three increasing values of β. The spectra of the three time series are also shown below. Forcing F and G in all three cases are the same. F has an annual cycle.

5. Modelling of the tropical surface winds

5.1. *Simulation of surface winds by a GCM*

The primary objective of the coupled models is to simulate the LF interannual variability such as the ENSO. Some recent studies[35, 27] have shown that the large-scale part of the observed surface winds represented by the first two or three empirical orthogonal functions (EOFs) is sufficient to force the observed interannual variability in an ocean model. These studies indicate that the small-scale high-frequency part of the surface winds is not essential in driving the LF interannual variability in the ocean. Based on these studies it appears that an atmospheric model that is successful in simulating the large-scale part of the surface winds accurately may be a good choice for the atmospheric component of a coupled model even if it does not simulate the HF component well. We shall analyse the results of an AGCM with this background in mind.

The model used in this study is a low-resolution version of the COLA (Center for Ocean Land Atmosphere Interactions, U. Maryland, USA) AGCM. It is a spectral model with R15 (rhomboidal truncation with 15 waves in the east–west direction) horizontal resolution and 18 discrete vertical levels. The model employs primitive equations of motion with divergence, vorticity, virtual temperature, water vapour and surface pressure as prognostic variables. The model contains parameterizations of most of the important physical processes, including a simple biosphere model (SiB) of Sellers *et al*[36]. The model has been integrated using the observed monthly mean SSTs from January 1979 to March 1992. The integration was initiated with the observed atmospheric data corresponding to January 1, 1979.

For comparison with observations we use the surface winds from the comprehensive ocean–atmosphere data set (COADS)[37] from January 1979 to December 1987. For the period between January 1988 and March 1992, we have used ECMWF (European Center for Medium-Range Forecasting) analysis at 1000 mb. As we are interested in the low-frequency variability, both the observed and the simulated winds are subjected to a five-month running mean filter. To compare simulated precipitation with observations, we have used the highly reflective cloud (HRC)[38] data between 1979 and 1987.

We have made detailed comparison of the simulated annual cycle of the surface winds as well as their interannual variations[39]. Here we present only one result (Fig. 12) that shows the evolution of the wind anomalies along the equator in the model simulations as well as in the observations. The simulated equatorial wind anomalies are of comparable magnitude to the observed anomalies. The model simulations capture the eastward propagation of the westerly wind anomalies during the warm episodes such as 81/82, 87/88 and 90/91.

The good simulation of the large-scale low-frequency part of the tropical surface winds seems to be related the model's ability to simulate the large-scale low-frequency part of the precipitation[39]. Good correspondence is found between the simulated precipitation and the highly reflective cloud (HRC) anomalies in the first two EOFs of the five-month running means. Moreover, the strong correlation between the simulated precipi-

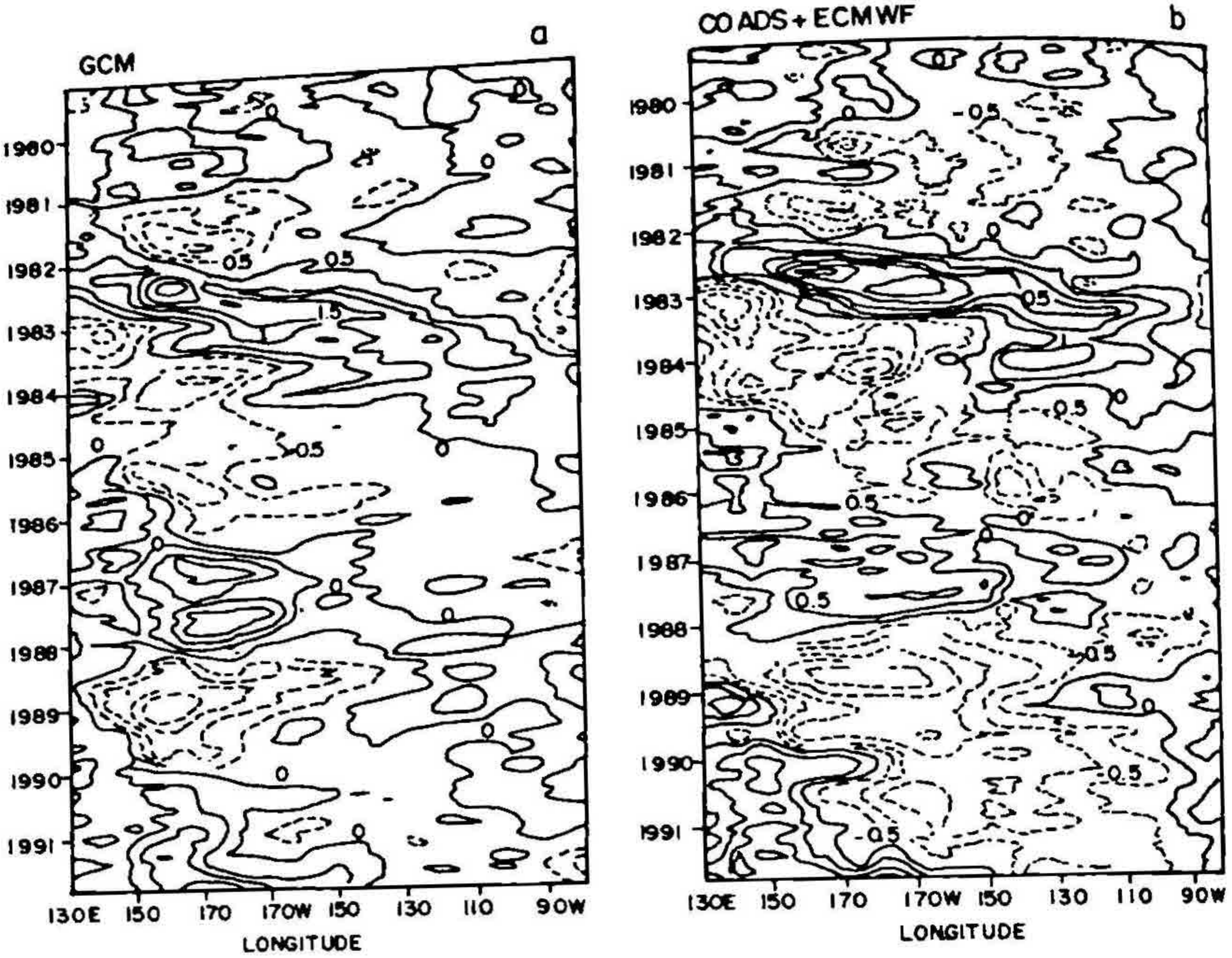

FIG. 12. Simulated and observed zonal winds averaged between 6°N and 6°S across the equatorial Pacific basin as a function of time. In (b) up to December 1987, COADS data are used. From January 1988 onwards, data from ECMWF analysis are used. Negative contours are dashed. Contour interval is 0.5 ms.

tation and the simulated winds in the first two principal components indicates the primary role of the precipitation in driving the surface winds. The surface winds simulated by a linear model forced by the GCM-simulated precipitation show[39] good resemblance with the GCM-simulated winds. This indicates that the tropical surface winds are governed primarily by linear dynamics.

5.2. *A linear model for tropical surface winds*

The surface winds in the tropics may be viewed as arising from two processes—the baroclinic response of the tropical troposphere to latent heat forcing by deep convection and the response to pressure gradients which develop hydrostatically in the turbulent atmospheric boundary layer due to the underlying SST. The first of these mechanisms was invoked by Gill[9] in a simple linear model for tropical surface winds. The role of the boundary-layer pressure gradients in producing surface winds was put forward by Lindzen and Nigam[40]. We argue that both these processes may be at work depending on

the background condition. For example, in the western Pacific the mean SST is high but the SST gradients are weak. This region is, therefore, favourable for deep convection but not for SST gradient-induced surface winds. On the other hand, in the eastern Pacific the mean SST is weak but the SST gradients are strong. Therefore, deep convection normally is rare here but the SST gradients could still produce enough surface winds. So it is argued that a model of tropical surface winds should include both these dynamical processes.

Secondly, we address the question of the importance of dynamical factors governing the maintenance of the observed surface winds in the tropics. Murphy and van den Dool[41] studied the momentum balance for the monthly mean surface winds and concluded that nonlinearity played only a minor role in the momentum balance. Zeibak[42] studied the vorticity budget of the monthly surface wind anomalies in the tropical Pacific and also concluded that the nonlinear advection terms are of second-order importance. He then proceeded to infer the forcing that may be required to drive the observed surface winds in a linear model by solving the inverse problem. The interesting result that emerged from this study was that the inferred forcing field was very different from the SST anomaly field but bore close resemblance to HRC anomalies that are representative of atmospheric heating anomalies. Thus, the problem with many simple linear models used in earlier studies to simulate the surface winds was not that they neglected the nonlinearities but that they parameterized the atmospheric heating wrongly. Most of these studies assumed atmospheric heating to be directly proportional to SST anomalies. Such a parameterization fails to simulate both the location and the horizontal scale of the atmospheric heating. For example, during a mature warm phase of ENSO, the SST anomaly maximum is located in the eastern part of Pacific while the atmospheric heating anomalies (as seen from the HRC anomalies) is maximum around the date line. Similarly, Neelin[43] showed (as we have also mentioned in the previous section) that if a linear model is forced by heating derived from the GCM-simulated precipitation field, it can simulate tropical surface winds that closely resemble the GCM-simulated surface winds in the tropics. All these studies indicate that a linear model may be sufficient for simulating the surface winds if the model can parameterize the atmospheric heating field correctly. However, the organized convective heating in the tropics is governed by nonlinear dynamical and thermodynamical processes. To parameterize it within the framework of a linear model is a daunting task!

We have proposed a new parameterization scheme for atmospheric heating for use in such simple models. This is an empirical scheme based on some recent observations. It has been known for some time that the relationship between tropical convection and SST is quite nonlinear[45,46]. Some recent studies[47–49] have established the relationship between SST and convection much more clearly. These studies have established that although at higher SST the variability of convection at a given SST increases, there is a clear nonlinear increase of convection with SST between SST > 26.5°C and less than or equal to 29.5°C. For SST > 29.5°C the convective activity drops off. We parameterize this relationship with the following empirical formula

$$\left.\begin{aligned} &\text{OLR}\ (\text{W m}^{-2}) = 260 && \text{SST} < 26.5^\circ\text{C}, \\ &\text{OLR}\ (\text{W m}^{-2}) = 260 - 35\left(\frac{\text{SST} - 26.5)}{3}\right)^2 && 26.5^\circ \le \text{SST} \le 29.5^\circ\text{C}, \\ &\text{OLR}\ (\text{W m}^{-2}) = 225, && \text{SST} > 29.5^\circ\text{C}. \end{aligned}\right\} \tag{6}$$

The quadratic relation gives an approximate fit to the nonlinear decrease of the outgoing longwave radiation (OLR) with SST, documented by Waliser *et al*[49]. We recall that OLR and precipitation may be related by another empirical formula[50]

$$\begin{aligned} P\ (\text{mm day}^{-1}) &= 48.38 - 0.186\text{OLR} \\ &= 6.5\left(\frac{\text{SST} - 26.5}{3}\right)^2, \quad 26.5^\circ\text{C} \le \text{SST} \le 29.5^\circ\text{C}. \end{aligned} \tag{7}$$

We note that for SST < 26.5°C, $P = 0$ and for SST > 29.5°C, $P = 6.5$ mm day^{-1}. From eqn (7) we can write

$$\frac{dP}{dT} = \frac{4.33}{3}(\text{SST} - 26.5).$$

This means that the precipitation rate for one degree increase in SST goes from 0 at SST = 26.5°C to a value of 4.33 mm day^{-1} K^{-1} at SST = 29.5°C. With this formulation for precipitation as a function of SST, we can write the heating function as

$$Q = \alpha P$$

where P is in mm day^{-1} and α has the dimensions of kg^{-3} mm^{-1} day. Using the thermodynamic and hydrostatic relations α can be estimated to be approximately 5.36 kg^{-3} mm^{-1} day. Thus, if we know SST, we can estimate the large-scale low-frequency part of the precipitation and hence the associated convective heating. We emphasize, however, that this formula may not work on a day-to-day basis.

The boundary layer response to the mid-tropospheric heating associated with the large-scale part of the organized deep convection is modelled by a Gill-type model,

$$\left.\begin{aligned} &u'_t - f v' + \phi'_x + \varepsilon u' = 0, \\ &v'_t + f u' + \phi'_y + \varepsilon v' = 0, \\ &\phi'_t + c^2(u'_x + v'_y) + \varepsilon\phi = -Q', \end{aligned}\right\} \tag{8}$$

where u' and v' are perturbations in the horizontal components of mass flux in the boundary layer, ϕ' is the mass-weighted integral of the perturbation geopotential height in the boundary layer, ε, the coefficient of Rayleigh friction, and f, the Coriolis parameter. Q' is the forcing function associated with the deep convection.

For the part of the boundary-layer flow due to pressure gradients arising from SST gradients, we use the Lindzen and Nigam[40] (hereafter referred to as LN) formulation

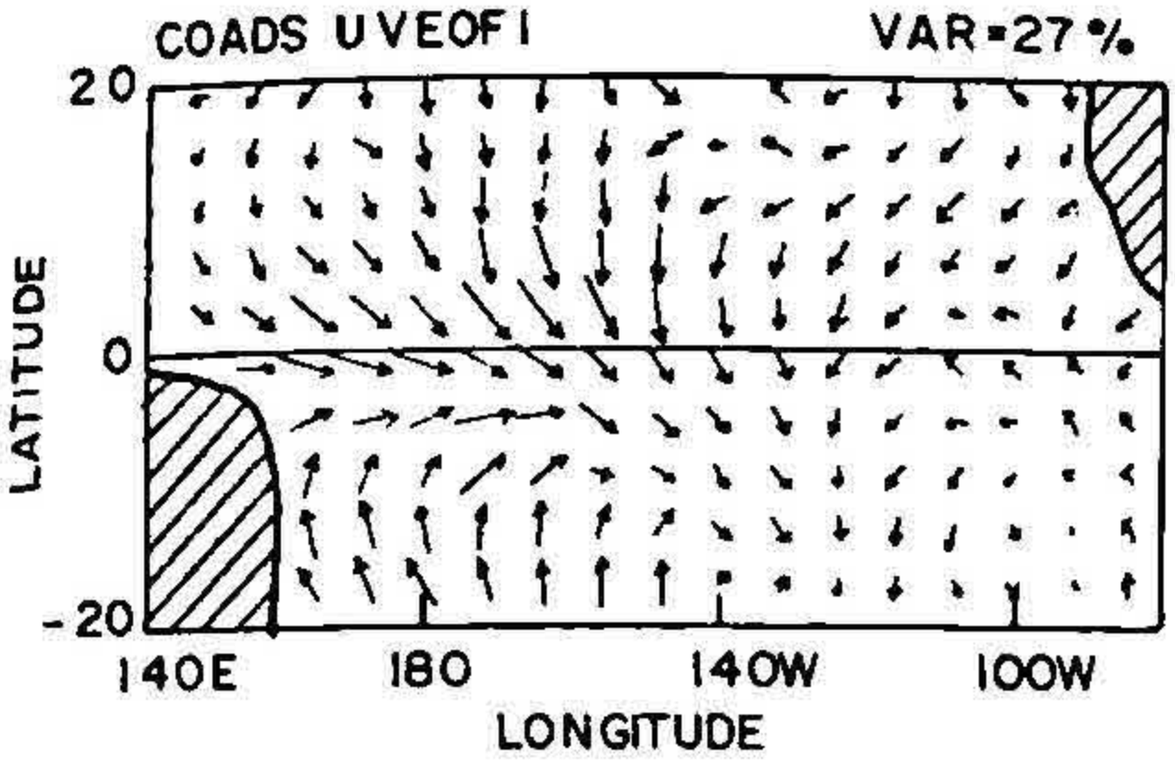

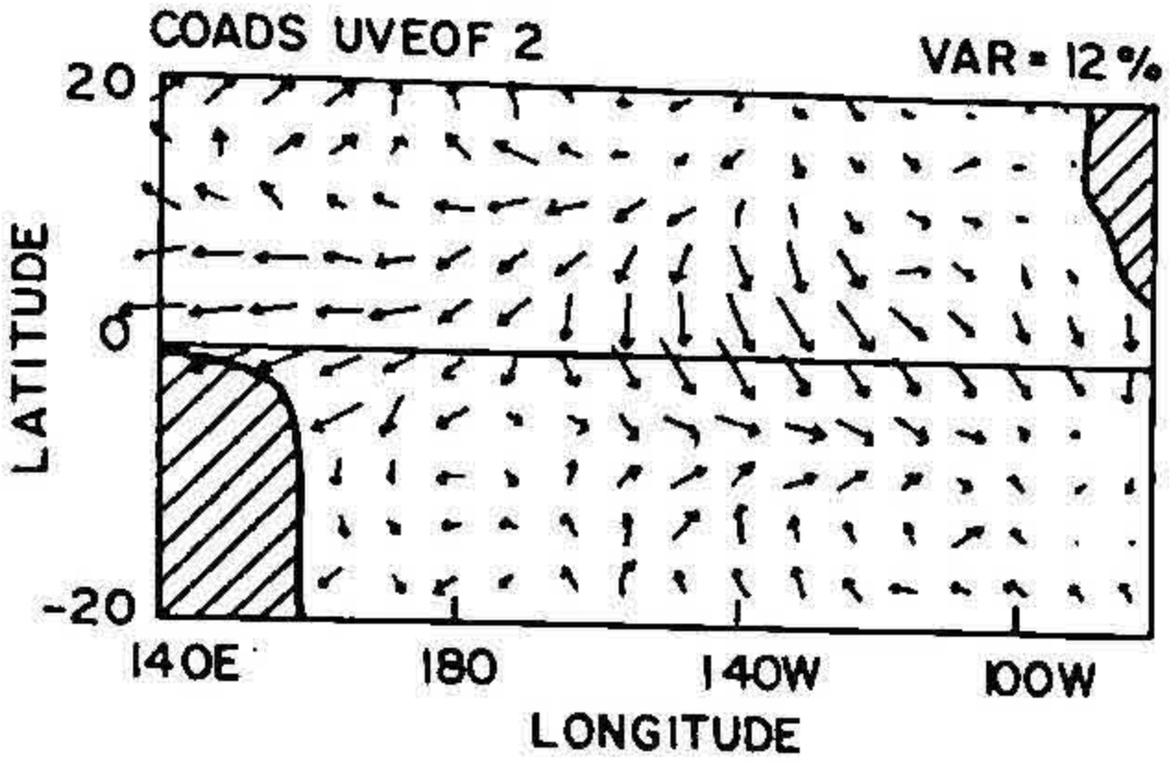

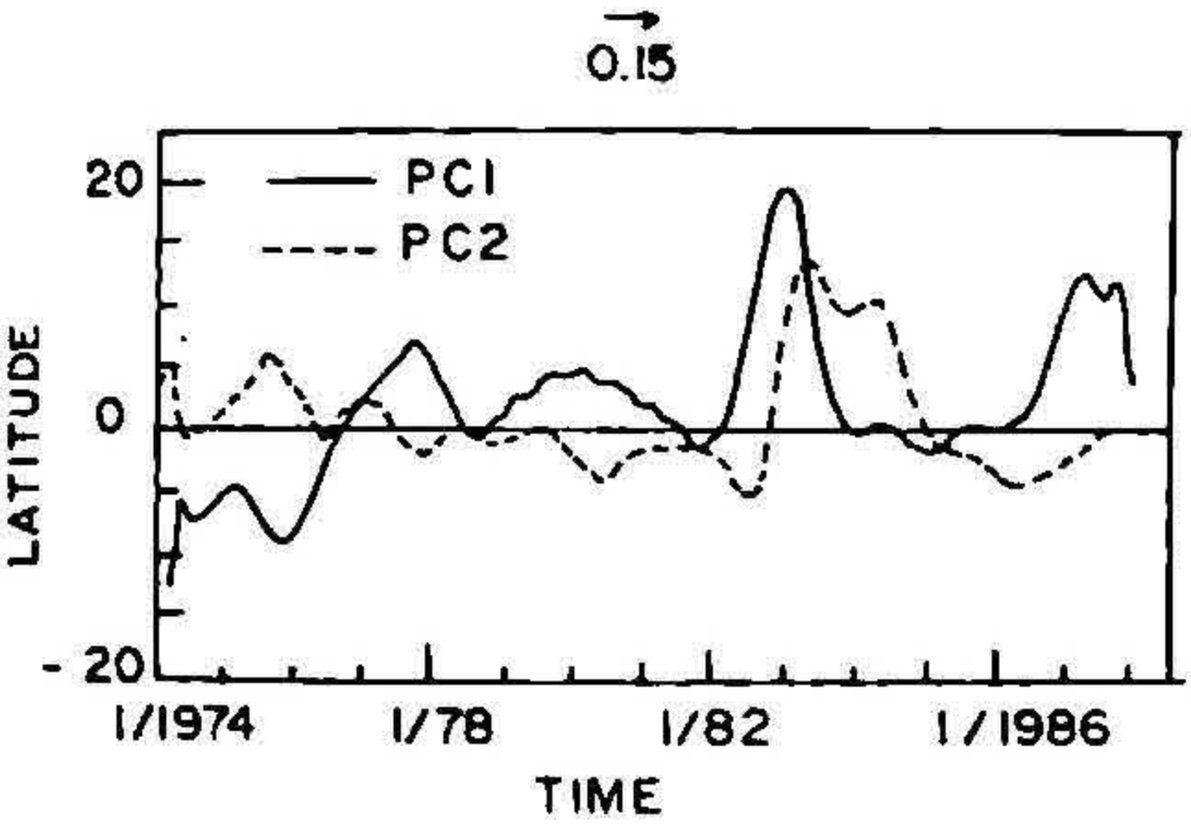

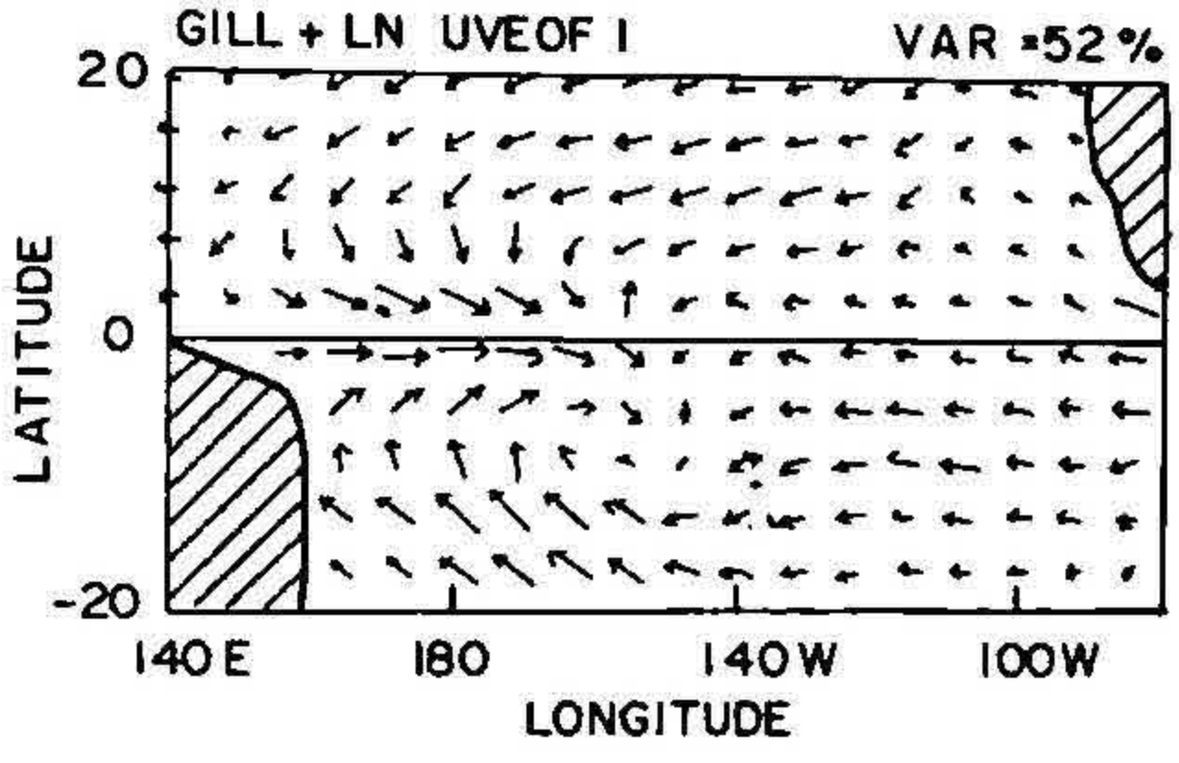

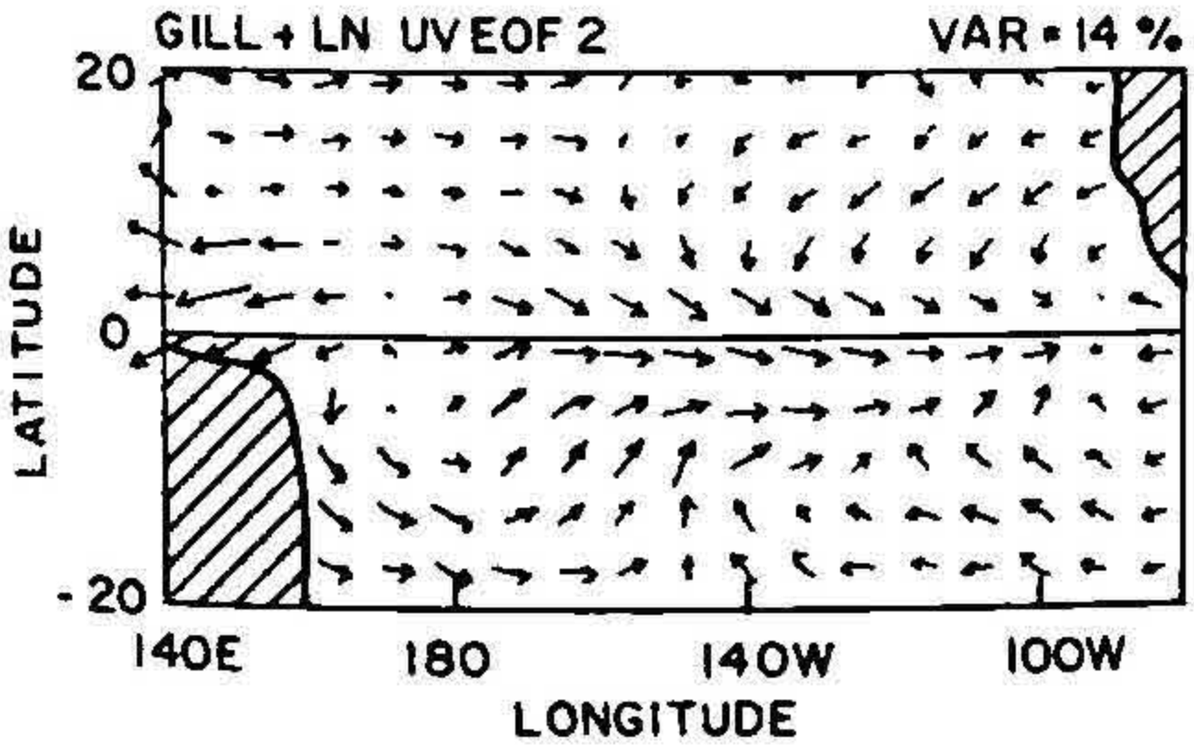

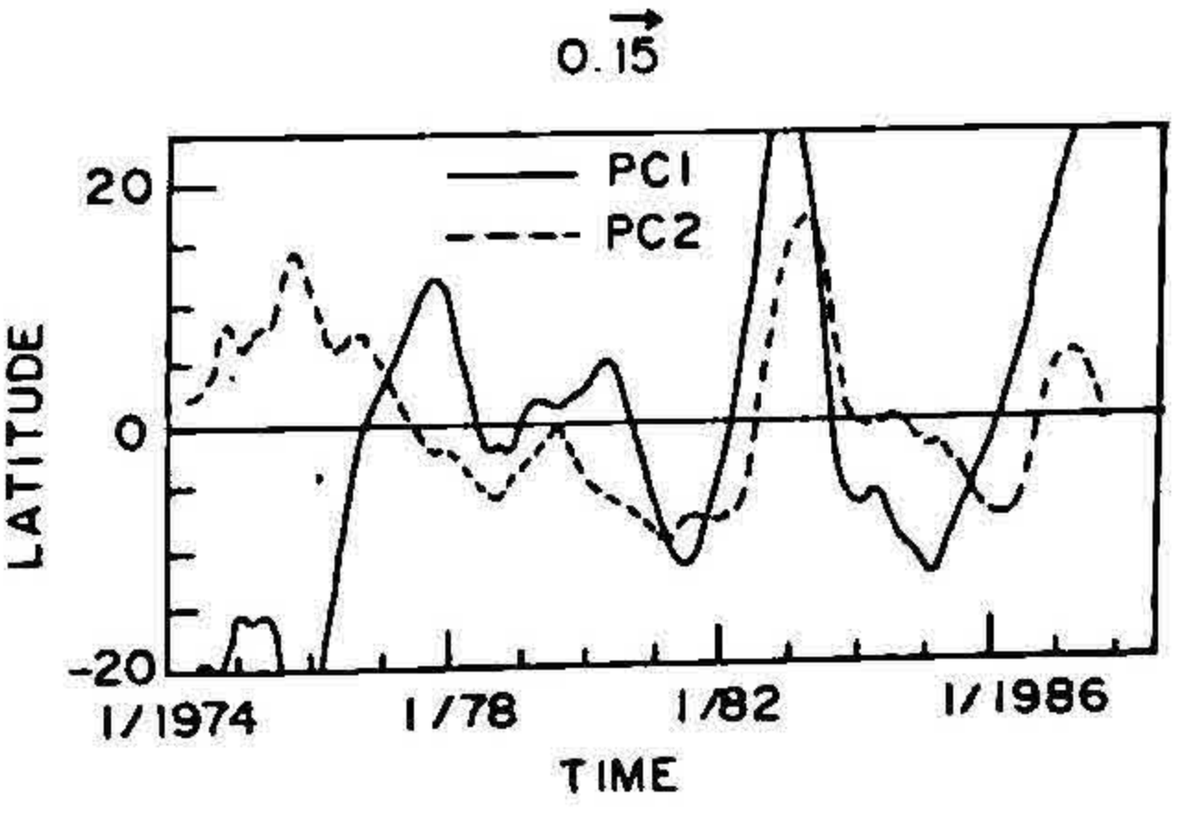

FIG. 13. The first two EOFs of the observed winds and their principal components are compared with those of the linear model-simulated winds. The negative contours are dashed.

with the back pressure effect. As Neelin[51] showed, the LN model could be transformed to the following form, which is similar to the Gill model:

$$\left.\begin{aligned} u_t' - fv' + \phi_x'' + \varepsilon u' &= 0, \\ v_t' + fu' + \phi_y'' + \varepsilon v' &= 0, \\ \phi'' + c^2(u_x' + v_y') + \varepsilon\phi'' &= Q' - bT_s'. \end{aligned}\right\} \tag{9}$$

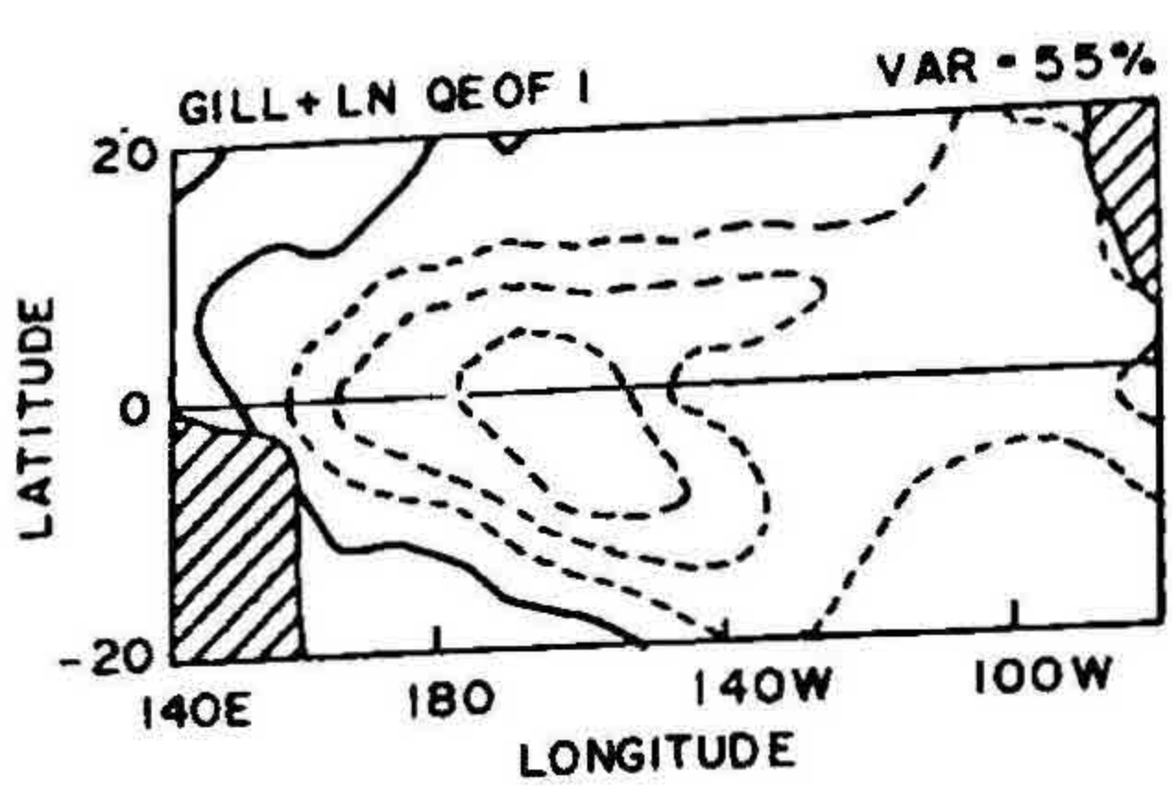

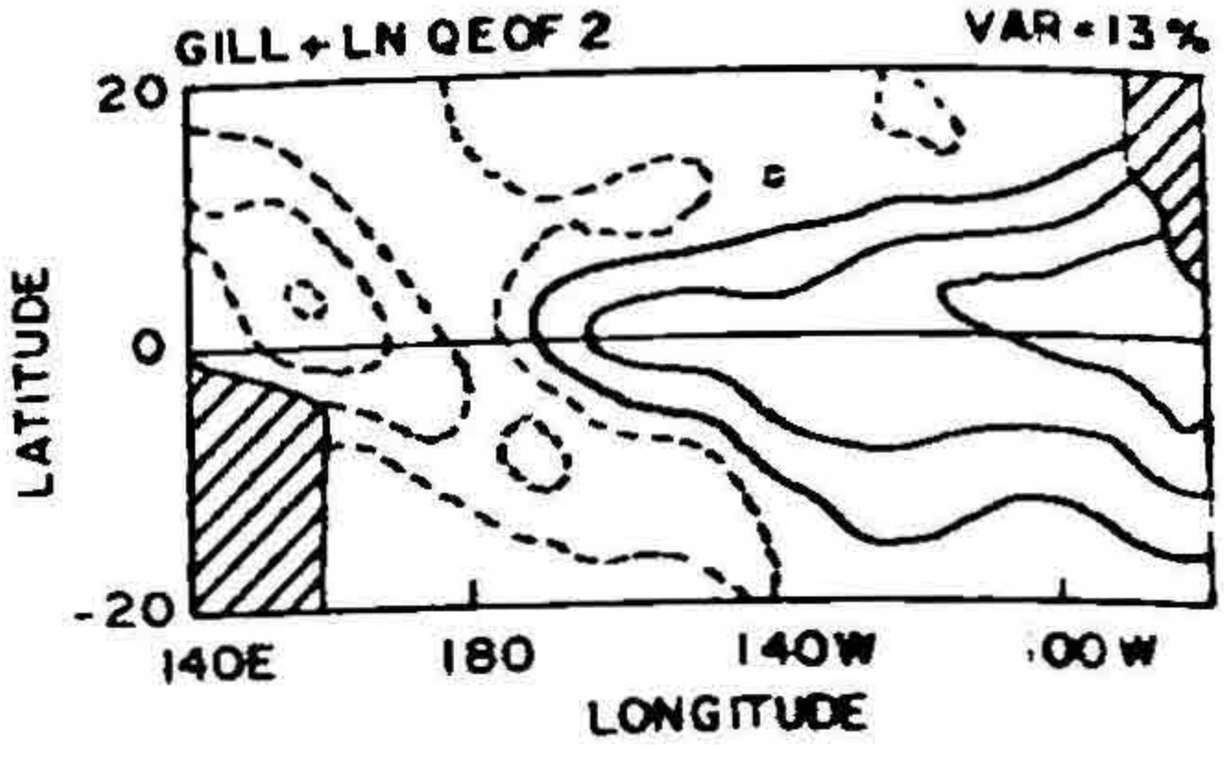

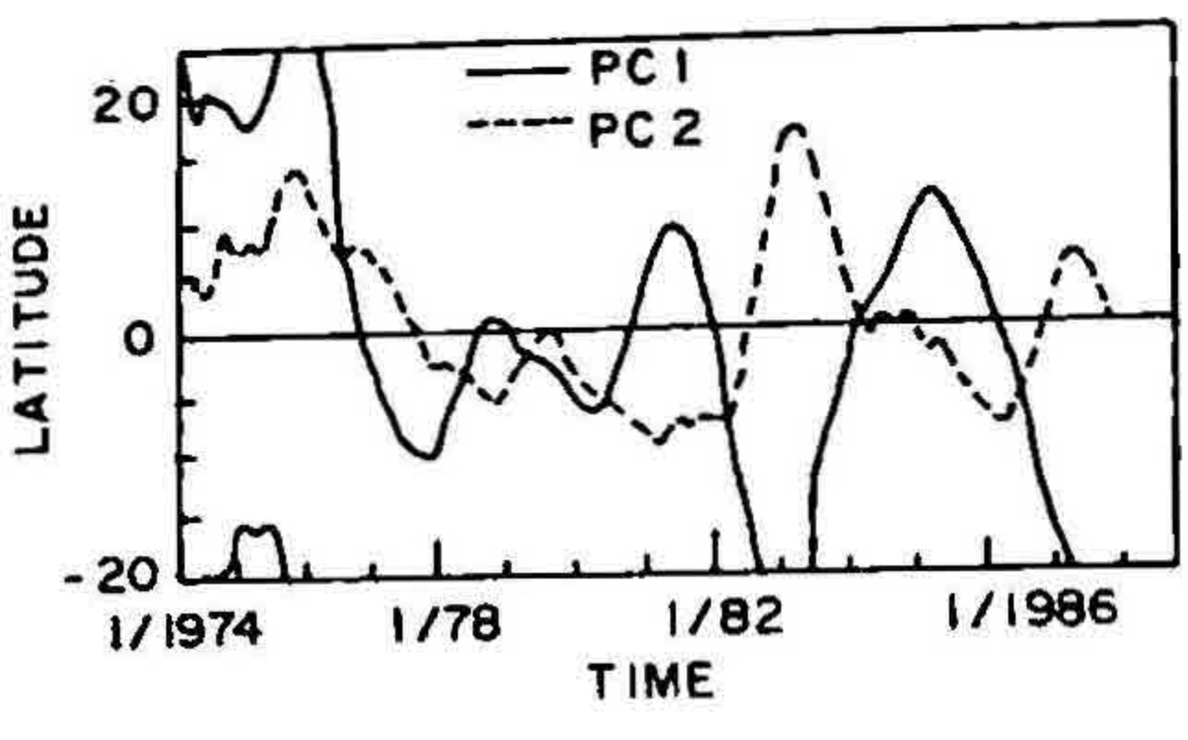

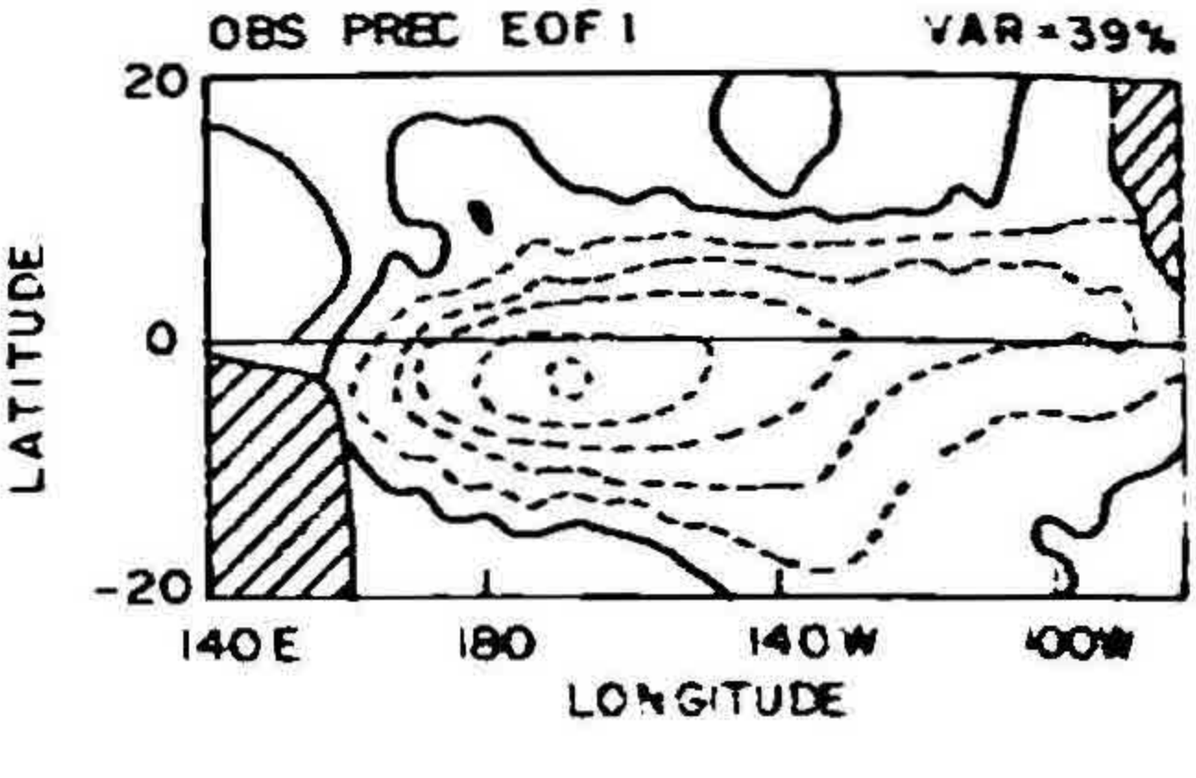

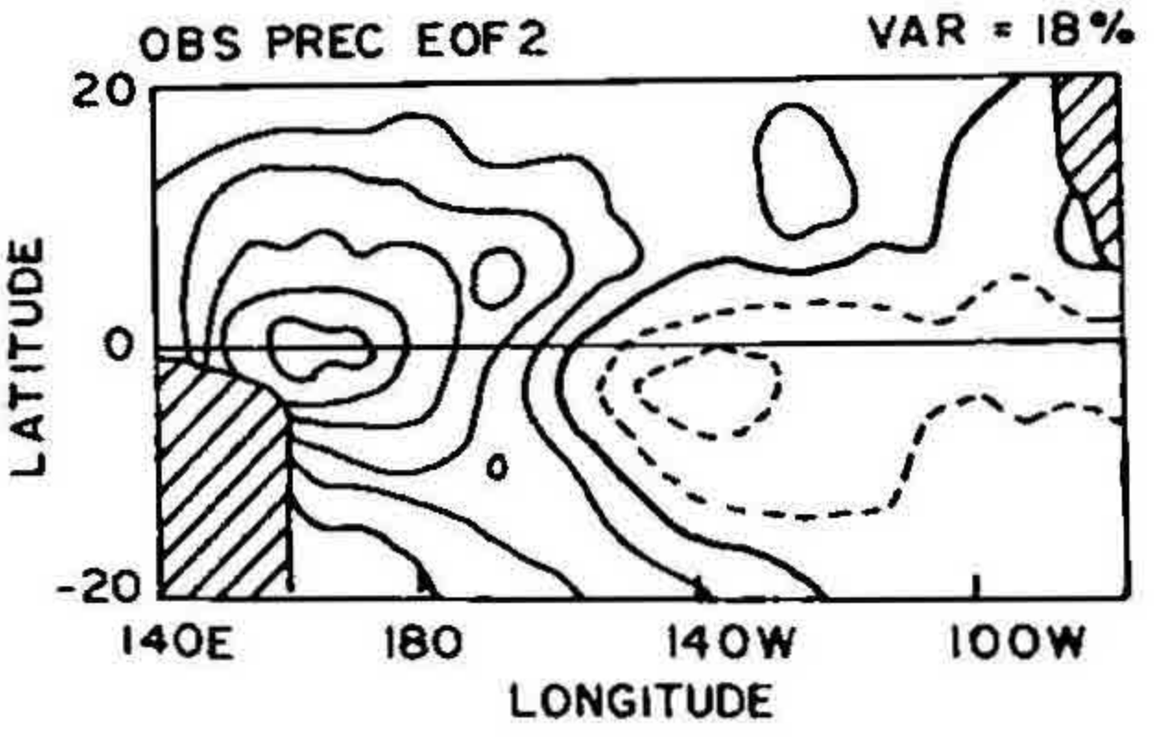

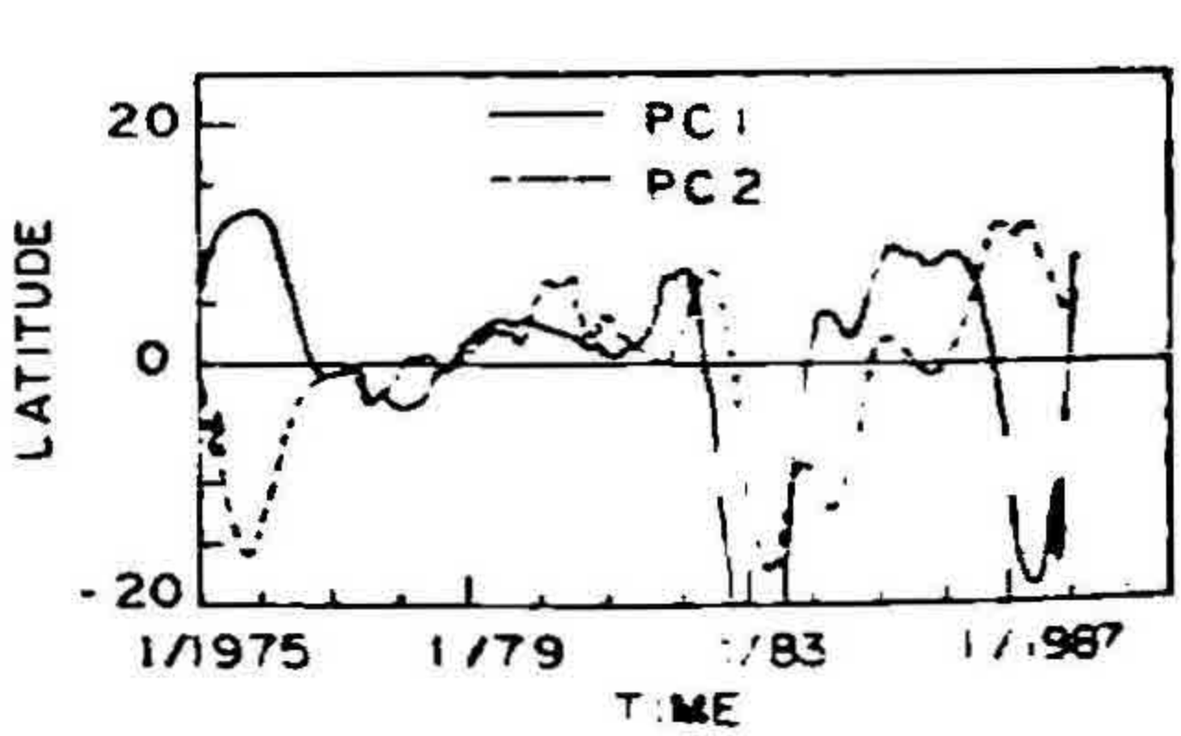

FIG. 14. The first two EOFs of the observed precipitation and their principal components are compared with those of the parameterized heating function for the linear model.

Here T_s' is the SST and $b = \varepsilon \delta P H_0 / 2T_0$, where δP is the depth of the boundary layer in units of pressure. H_0 is the depth of the boundary layer in units of length and T_0 is a onstant reference temperature ($T_0 = 288$ K). $\phi'' = g(h' - H_0/2T_0)T_s'$, where h' is the perturbation height of the boundary layer.

We exploit the similarity and linearity of eqns (8) and (9) to combine them to the following set of equations:

$$\left.\begin{aligned} &u'_t - fv' + \phi'''_x + \varepsilon u' = 0, \\ &v'_t + fu' + \phi'''_y + \varepsilon v' = 0, \\ &\phi'''_t + c^2(u'_x + v'_y) + \varepsilon\phi''' = Q' - bT'_s. \end{aligned}\right\} \quad (10\text{ a, b, c})$$

where $\phi''' = \phi' + \phi''$.

In this manner, our linear model of the tropical boundary layer represented by eqns (10) contains both the important forcings, one arising from heat released in deep convection (represented by Q') and the other associated with SST gradients (represented by bT_s'). Using the observed SST from COADS, the total heating for each month is calculated using our parameterization, discussed earlier in this section. From these heatings, climatological mean heating corresponding to each calendar month is calculated and by subtracting it from the individual monthly estimates, anomalous heating for individual months is computed. The linear model is forced by the combined forcing. The Rayleigh friction coefficient used in our model is $(2\text{ days})^{-1}$. This way mean monthly surface wind anomalies are simulated[44] from January 1974 to December 1987. The first two EOFs of the simulated winds are shown in Fig. 13 and are compared with those of the observed surface winds for the same period. It is seen that the large-scale pattern is quite well simulated. Noteworthy is the correct simulation of the location of the westerly anomalies during a warm event. The good simulation of the first of two EOFs of the surface winds is related to the good simulation of the first two EOFs of the deep convective heating by our parameterization as shown in Fig. 14. To gain further insight, we show in Fig. 15 that the time longitude section of the equatorial zonal wind anomalies averaged between 5 N and 5 S. It is seen from this figure that the model does a good job of simulating the eastward migration of westerly anomalies during 1982–1983, the easterly anomalies during 1974–1975, the westerly anomalies during 1986–1987. The simulation of the large-scale part of the surface winds by our simple model is comparable to that of even some GCMs. We also examined the contributions made by deep convective heating as well as the SST gradients. We find[44] (not shown) that the convective heating is mainly responsible for driving the surface winds in the western Pacific while the SST gradients make appreciable contribution to the surface winds in the eastern Pacific.

4. Conclusions

Extensive experiments with a coupled ocean–atmosphere model provides the first quantitative estimate on the limit on the predictability of the coupled system. Further investigation with the coupled model, theoretical stability analysis with a linear coupled model have shown that increase in atmospheric heating associated with anomalous surface convergence (convergence feedback) results in the coexistence of an LF longwave mode with a host of IS shortwave modes. A conceptual model is then constructed that illustrates how nonlinear interactions between the LF mode and the IS modes could lead to the observed aperiodicity in the coupled system. These results provide the foundation for predictability studies of the tropical climate. Our current work involves attempts to identify initial conditions that support either the fast or the slow growth of errors and to find ways of suppressing the former.

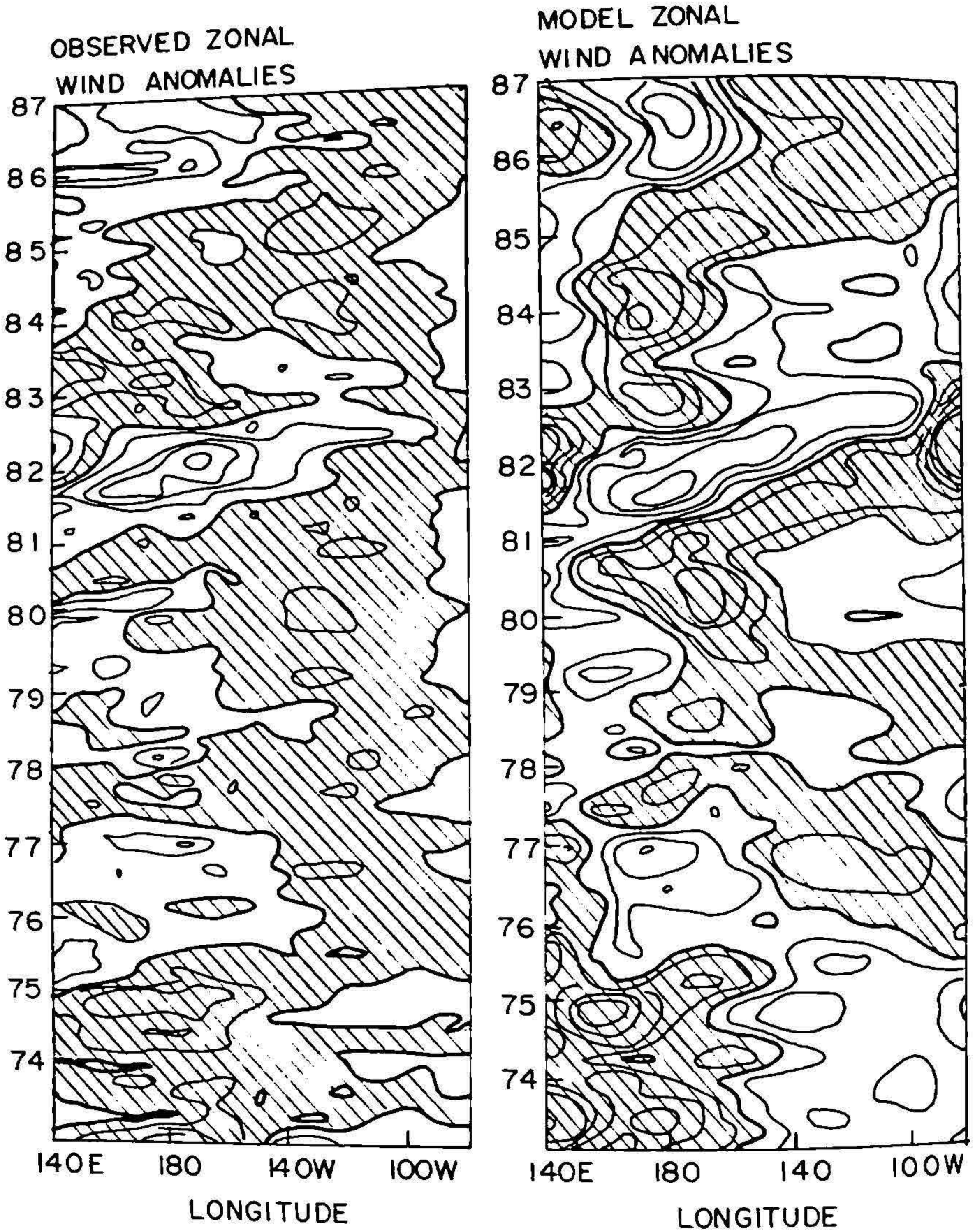

FIG. 15. Time-longitude sections of the observed and linear model-simulated zonal wind anomalies along the equatorial Pacific averaged between 5°N and 5°S.

For coupled modelling studies, the atmospheric component is required to simulate the large-scale part of the observed surface winds accurately as only this part is responsible for driving low-frequency interannual variability in the oceans. An improved linear atmospheric model is developed for simulating the large-scale component of the observed surface wind variability. The model is tested over the Pacific Ocean for the period 1974–1987. The first two empirical orthogonal functions of the surface winds simulated by the model agree remarkably well with the corresponding EOFs of the observed surface winds. The model not only captures the large-scale low-frequency part of the surface winds given by the first two EOFs, it also successfully simulates the equatorial surface wind anomalies and their evolution during the entire period 1974–1987. The noteworthy success of this simple model stems from two improvements on existing linear models. First, the model incorporates the driving of surface winds both by deep convection and by sea surface temperature (SST) gradients. Secondly, it contains a new improved parameterization of organized deep convection. The parameterization is based on observations which show that there is a threshold in SST below which organized deep convection rarely occurs and above which organized deep convection increases nonlinearly with SST. It is shown that this parameterization is successful in simulating the large-scale part of the observed precipitation anomalies quite well. It is also shown that the convective heating is mainly responsible for driving surface winds in the western and central Pacific, while the SST gradients contribute in a subtle way in driving surface winds in the eastern Pacific. The simulation of the large-scale part of the surface winds by our simple model is comparable to those by many GCMs. This makes the present low-cost model an attractive choice for modelling studies.

Acknowledgements

The results presented here owe their origin to several studies conducted at the Centre for Atmospheric Sciences, Indian Institute of Science, Bangalore, in collaboration with V. Krishnamurthy, Sudha Selvarajan and N. H. Saji. The author thanks Anna Valerio of Program in Atmospheric and Oceanic Sciences of Princeton University for her expert preparation of the manuscript. This work is partly supported by a grant from the Department of Science and Technology, Government of India.

References

1. LORENZ, E. N. — A study of predictability of a 28-variable atmospheric model. *Tellus*, 1965, 17, 321–333.

2. CHARNEY, J. G. AND SHUKLA, J. — Predictability of monsoon. In *Monsoon dynamics* (Sir James Lighthill and R. P. Pearce (eds)), pp. 99–110, 1981, Cambridge University Press.

3. RASMUSSON, E. M. AND CARPENTER, T. H. — Variations in tropical sea surface temperature and sea surface wind fields associated with the Southern Oscillation/El Nino. *Mon. Weath. Rev.*, 1982, 110, 354–384.

4. BJERKNES, J. — Atmospheric teleconnections from the equatorial Pacific. *Mon. Weath. Rev.*, 1969, 97, 163–172.

5. PHILANDER, S. G. H., YAMAGATA, T. AND PACANOWSKI, R.C. — Unstable air–sea interactions in the tropics, *J. Atmos. Sci.*, 1984, 41, 604–613.

6. HIRST, A. C. — Unstable and dumpled equatorial models, *J. Atmos. Sci.*, 1986, 43, 606–630.

7. GOSWAMI, B. N. AND SELVARAJAN, S. — Convergence feedback and unstable low frequency oscillations in a simple coupled ocean–atmosphere model, *Geophys. Res. Lett.*, 1991, 18, 991–994.

8. WEBSTER, P. — Response of the tropical atmosphere to local, steady forcing, *Mon. Weath. Rev.*, 1972, 100, 518–541.

9. GILL, A. C. — Some simple solutions of heat-induced tropical circulations, *Q. J. R. Met. Soc.*, 1980, 106, 447–462.

10. CANE, M. A. AND SARCHIK, E. S. — Forced baroclinic ocean motions. I: The linear equatorial unbounded case, *J. Mar. Res.*, 1976, 34, 233–252.

11. CANE, M. A. AND SARACHIK, E. S. — Forced baroclinic ocean motions. II: The linear equatorial bounded case, *J. Mar. Res.*, 1977, 35, 395–432.

12. CANE, M. A. AND SARACHIK, E. S. — Forced baroclinic ocean motions. III: The linear equatorial basin case, *J. Mar. Res.*, 1979, 37, 355–398.

13. BATTISTI, D. S. AND HIRST, A. C. — Interannual variability in the tropical atmosphere/ocean system: Influence of the basic state and ocean geometry, *J. Atmos. Sci.*, 1989, 46, 1687–1712.

14. LAU, N. C. — Modelling the seasonal dependence of atmospheric response to observed El Nino in 1962–76, *Mon. Weath. Rev.*, 1985, 113, 1970–1996.

15. BUSALLACCHI, A. J. AND O'BRIEN, J. — Interannual variability of the equatorial Pacific in the 1960s, *J. Geophys. Res.*, 1981, 86, 10901–10907.

16. ZEBIAK, S. E. AND CANE, M. A. — A model El Nino–Southern Oscillation, *Mon. Weath. Rev.*, 1987, 115, 2262–2278.

17. PHILANDER, S. G. H., PACANOWSKI, R. C., LAU, N. C. AND NATH, M. J. — Simulation of ENSO with a global atmospheric GCM coupled to a high-resolution tropical Pacific ocean GCM, *J. Climate*, 1992, 5, 308–329.

18. LAU, N. C., PHILANDER, S. G. H. AND NATH, M. J. — Simulation of ENSO-like phenomena with a low-resolution coupled GCM of the global ocean and atmosphere, *J. Climate*, 1992, 5, 284–307.

19. LATIF, M., STERL, A., MAIER–REIMER, E. AND JUNGE, M. M. — Climate variability in a coupled GCM. Part I: The tropical Pacific, *J. Climate*, 1993, 6, 5–21.

20. NEELIN, D., *et al.* — Tropical air–sea interactions in general circulation models, *Clim. Dynam.*, 1992, 7, 73–104.

21. GOSWAMI, B. N. — Ocean–atmosphere coupled models and dynamics of ENSO. In *Advances in tropical meteorology, monsoon variability – Satellite applications and modelling*, (R. N. Keshavamurthy and P. C. Joshi, (eds)), pp. 401–412, 1994, Tata McGraw-Hill, New Delhi.

22. CANE, M. A. AND ZEBIAK, S. E. — Experimental forecasts of El Nino, *Nature*, 1986, 321, 827–832.

23. BARNETT, T. P. — On the prediction of the El Nino of 1986–87, *Science*, 1988, 241, 192–196.

24. SUAREZ, M. J. AND SCHOPF, P. S. A delayed oscillator for ENSO, *J. Atmos. Sci.*, 1988, 46, 3283–3287.

25. BATTISTI, D. S. AND HIRST, A. C. Interannual variability in the tropical atmosphere–ocean system: Influence of the basic state and ocean geometry, *J. Atmos. Sci.*, 1989, 46, 1687–1712.

26. LATIF, M. AND FLUGEL, M. An investigation of short-range climate predictability in the tropical Pacific, *J. Geophys. Res.*, 1991, 96, 2661–2673.

27. GOSWAMI, B. N. AND SHUKLA, J. Predictability of a coupled ocean–atmosphere model, *J. Climate*, 1991, 4, 3–22.

28. GOSWAMI, B. N. AND SHUKLA, J. Aperiodic variability in the Cane–Zebiak model: A diagnostic study, *J. Climate*, 1993, 6, 628–638.

29. GOSWAMI, B. N. AND SELVARAJAN, S. Convergence feedback and unstable low-frequency oscillations in a simple coupled ocean–atmosphere model, *Geophys. Res. Lett.*, 1991, 18, 991–994.

30. SELVARAJAN, S. AND COSWAMI, B. N. On the stability of a coupled ocean–atmosphere system in the presence of wave–CISK, *Proc. Indian Acad. Sci. (Earth Planet. Sci.)*, 1992, 101, 153–176.

31. GOSWAMI, B. N., SELVARAJAN, S. AND KRISHNAMURTHY, V. Mechanisms of variability and predictability of the tropical coupled ocean–atmosphere system, *Proc. Indian. Acad. Sci. (Earth Planet. Sci.)*, 1993, 102, 49–72.

32. KRISHNAMURTHY, V. GOSWAMI, B. N. AND LEGNANI, R. A conceptual model for the aperiodicity of interannual variability in the tropics, *Geophys. Res. Lett.*, 1993, 20, 435–438.

33. LORENZ, E. N. Irregularity, a fundamental property of the atmosphere, *Tellus A*, 1984, 36, 98–110.

34. GOSWAMI, B. N. A multiscale interaction model for the origin of the tropospheric QBO, *J. Climate*, 1995, 8, 524–534.

35. LATIF, M., BIERCAMP, J., STORCH, H. V. AND KIRK, E. Simulation of ENSO-related surface wind anomalies with an atmospheric GCM forced by observed SST, *J. Climate*, 1990, 3, 509–521.

36. SELLERS, P. J., MINTZ, Y., SUD, Y. C. AND DALCHER, A. A simple biosphere model (SiB) for use within general circulation models, *J. Atmos. Sci.*, 1986, 43, 505–531.

37. SLUTZ, R. J. *et al.* *Comprehensive ocean–atmosphere data set: Release 1*, NOAA Environmental Research Program, Boulder, Co, 1985, p. 268.

38. GARCIA, O. Atlas of highly reflective clouds for global tropics: 1971–1987, U.S. Department of Commerce, NOAA Environmental Research Laboratory, 1985.

39. GOSWAMI, B. N., KRISHNAMURTHY, V. AND SAJI, N. H. Simulation of ENSO-related surface winds in the tropical Pacific by an AGCM forced by observed SST, *CAS Technical Report No. 94 AS4*, Centre for Atmospheric Sciences, Indian Institute of Science, Bangalore, 1994.

40. LINDZEN, R. S. AND NIGAM, S. On the role of sea surface temperature gradients in forcing low-level winds in the tropics, *J. Atmos. Sci.*, 1987, 45, 2440–2458.

41 MURPHREE, T. AND VAN DEN DOOL, H. Calculating winds from time mean sea level pressure fields, *J. Atmos. Sci.*, 1988, 45, 3269–3281.

42. ZEBIAK S. E. Diagnostic study of Pacific surface winds, *J. Climate*, 1990, 3, 1016–1031.

43. NEELIN, J. D. — A simple model for surface stress and low level flow in the tropical atmosphere driven by prescribed heating. *Q. J. R. Met. Soc.*, 1988, 114, 747–770.

44. SAJI, N. H. AND GOSWAMI, B. N — An improved linear model of tropical surface wind variability. *Q. J. R. Met. Soc.*, 1995 (in press).

45. GADGIL, S., JOSEPH, P. V. AND JOSHI, N. V. — Ocean–atmosphere coupling over monsoon regions. *Nature*, 1984, 312, 141–143.

46. GRAHAM, N. E. AND BARNETT, T. P. — Sea surface temperature, surface wind divergence and convection over tropical oceans. *Science*, 1987, 238, 657–659.

47. FU, R. DELGENIO, A. D. AND ROSSOW, W. B. — Behaviour of deep convective clouds in the tropical Pacific deduced from ISCCP radiances. *J. Climate*, 1990, 3, 1129–1152.

48. ZHANG, C. — Large-scale variability of atmospheric deep convection in relation to sea surface temperature in the tropics. *J. Climate*, 1993, 6, 1898–1913.

49. WALISER, D. GRAHAM, N. E. AND GAUTIER, C. — Comparison of highly reflective cloud and outgoing longwave radiation data sets for use in estimating tropical deep convection. *J. Climate*, 1993, 6, 331–353.

50. YOO, J. M. AND CARTON, J. M. — Spatial dependence of the relationship between rainfall and outgoing longwave radiation in the tropical Atlantic. *J. Climate*, 1988, 1, 1047–1054.

51. NEELIN, J. D. — On the interpretation of the Gill model. *J. Atmos. Sci.*, 1989, 46, 2466–2468.

IISc Theses Abstracts

Contents